International Journal of Molecular Sciences

MDPI

Article

Automated microscopic measurement of fibrinaloid microclots and their degradation by nattokinase, the main natto protease

Justine M. Grixti[1], Chrispian W. Theron[1,2], J. Enrique Salcedo-Sora[1,2], Etheresia Pretorius[1,3*] & Douglas B. Kell[1,2,3,4*]

[1] Department of Biochemistry, Cell and Systems Biology, Institute of Systems, Molecular and Integrative Biology, Faculty of Health and Life Sciences, University of Liverpool, L69 7ZB, UK. {Justine.grixti}{c.theron}{j.salcedo-sora}{dbk}@liverpool.ac.uk

[2] Gene Mill Biofoundry, Institute of Systems, Molecular and Integrative Biology, Faculty of Health and Life Sciences, University of Liverpool, L69 7ZB, UK.

[3] Department of Physiological Sciences, Faculty of Science, Stellenbosch University, Stellenbosch, Private Bag X1 Matieland, 7602, South Africa; resiap@sun.ac.za ORCID: 0000-0002-9108-2384

[4] The Novo Nordisk Foundation Centre for Biosustainability, Technical University of Denmark, Søltofts Plads 220, 2800 Kgs Lyngby, Denmark. ORCID: 0000-0001-5838-7963

* Correspondence: dbk@liv.ac.uk; resiap@sun.ac.za

Abstract: Nattokinase, from the Japanese fermented food natto, is a protease with fibrinolytic activity that can thus degrade conventional blood clots. In some cases, however, including in Long COVID, fibrinogen can polymerise into an anomalous amyloid form to create clots that are resistant to normal fibrinolysis and that we refer to as fibrinaloid microclots. These can be detected with the fluorogenic stain thioflavin T. We describe an automated microscopic technique for the quantification of fibrinaloid microclot formation, which also allows the kinetics of their formation and aggregation to be recorded. We also here show that recombinant nattokinase is effective at degrading the fibrinaloid microclots *in vitro*. This adds to the otherwise largely anecdotal evidence, that we review, that nattokinase might be anticipated to have value as part of therapeutic treatments for individuals with Long COVID and related disorders that involve fibrinaloid microclots.

Keywords: Microclots – fibrinaloid – chronic disease – fibrinolysis – nattokinase – Long COVID

1. Introduction

Thrombosis, the blocking of blood vessels by blood clots, along with the related thrombo-inflammation and thromboembolism, is a chief cause of cardiovascular disease [1-6]. Consequently anything that can promote safe anti-coagulation or fibrinolytic activity is likely to have therapeutic potential (e.g. [7-15]).

Nattō (usually rendered natto) is a Japanese food made via the fermentation of soy beans using the Gram-positive organism *Bacillus subtilis* var natto [16-20]. It has been widely consumed for over 2000 years, and is considered safe [21]. The proteolytic activity of natto was detected in 1906 [22] and its fibrinolytic activity in 1925 [23]. However, it was not until 1987 [21] that an enzyme exhibiting these activities was purified from natto; in spite of it being a protease it was termed nattokinase [21].

Despite having to pass through the gut wall [24-31], nattokinase is orally available (and this can be improved [32-34]), is considered a major contributor to the purported health benefits of natto [21,27,35-60], and is itself recognised as safe [61-63].

Citation: To be added by editorial staff during production.

Academic Editor: Firstname Lastname

Received: date
Revised: date
Accepted: date
Published: date

The experimental 3D structure of nattokinase, which is a serine protease related to subtilisin, is available [64,65], and it may also be produced via purification [66-69] or (as here) recombinantly [44,70-83]. Although not our prime focus in this paper, it is also known to cleave plasminogen activator inhibitor I [84], to have antiplatelet [85], anti-inflammatory [86], and anti-hypertensive [87-89] activities, and to show neuroprotective [90] and post-stroke benefits [91] as well, when dosed adequately, as having anti-lipidaemic effects [92].

Following earlier work using electron microscopy (e.g. [93-96]), we discovered that fibrinogen could polymerise or clot into an anomalous, amyloid form of fibrin (e.g. [97-104]) that exactly reflected the clots seen in both the electron microscope [105] and in bright field optical microscopy [106]. As with prions and other amyloid forms of proteins [98,107], that are often highly resistant to proteolysis (e.g. [108,109]), the existence of these 'fibrinaloid' microclots implies their comparative resistance to normal fibrinolysis [110,111], with their precise structures [112] being affected by other small and macromolecules and ions that they may have bound [97,103,113-119]. The varieties of stable macrostates into which a given amyloidogenic sequence can fold (even under the same conditions [120,121]) are referred to as different 'strains' [122-132] or 'polymorphisms' [133-144], and in some cases are sufficiently stable (i.e. kinetically isolated from other macrostates) that they are even heritable [122,145-151]. Homo- and hetero-polymerisation and their catalysis are then referred to, respectively, as (self-)'seeding' [140,152-166] and 'cross-seeding' [153,167-174]. More recently, we have established the prevalence of these fibrinaloid microclots in post-viral diseases such as Long COVID [106,175-178] (and see [179]) and ME/CFS (myalgic encephalopathy/chronic fatigue syndrome) [180,181]. The lower amyloidogenicity of omicron versus earlier variants of SARS-CoV-2 is also reflected in its lower virulence [182], implying that these microclots are on the aetiological pathway of the disease, and they can explain many symptoms [183], including fatigue [184], post-exertional symptom exacerbation [185], autoantibody generation [107] and Postural Orthostatic Tachycardia Syndrome (POTS) [186]. Fibrin amyloid microclots also occur during sepsis [187], while amyloid deposits are also observed in the skeletal muscles of those with Long COVID [188]. Overall, this ability of fibrinaloid microclots to provide a mechanistic explanation of multiple phenomena is consistent with the 'explanatory coherence' view of science [189-192]. In common with other amyloid proteins [98], that contain a characteristic cross-β motif [173,193-209], they can be visualized using the fluorogenic stain thioflavin T [144,173,210-224] or via vibrational spectroscopy [221,225-236]. As with any other ligand or binding agent, the rotation of the bound form is more restricted than that of the free form (which is largely what makes it fluorogenic), and precise intensities of thioflavin T fluorescence depend on the location and conformation(s) to which the thioflavin T is bound [212-214,237-254] and in some cases on the presence of interferents [255].

Although nattokinase preparations are widely available commercially, and as noted above they are considered to have significant therapeutic value, including in Long COVID [256,257], their exact contents are uncertain, and so we decided that it was best to create and use purified, recombinant material.

While the proteolytic specificity of nattokinase, as an alkaline serine protease [44,258,259], is surprisingly underexplored, beyond a broad similarity to that of plasmin [44,260] (and nattokinase can even degrade spike protein [261] and certain 'classical' amyloids [262-264]), the question arises as to whether or not nattokinase can degrade the amyloid 'fibrinaloid' form of microclots. The purposes of this paper are (i) to describe an efficient, quantitative, automated microscopic method that can be used to determine the size and number of amyloid microclots and any time-dependent changes therein, and thus (ii) to assess any such nattokinase-induced degradation of the microclots,

84 concluding that nattokinase can indeed degrade fibrinaloid microclots effectively. The therapeutic implications of this
85 are discussed.

86 ## 2. Results

87 ### Basic phenomenon, and effect of concentration of NK and incubation time

88 To give an indication of the kinds of data obtained in this study, Figure 1 (left panels) shows three Cytation images
89 representing clots as stained with thioflavin T following incubation of fibrinogen plus thrombin plus LPS (as in [97])
90 for 6h, either with no further additions (Figure 1A, top), with PBS (Figure 1B, middle), or after simultaneous exposure

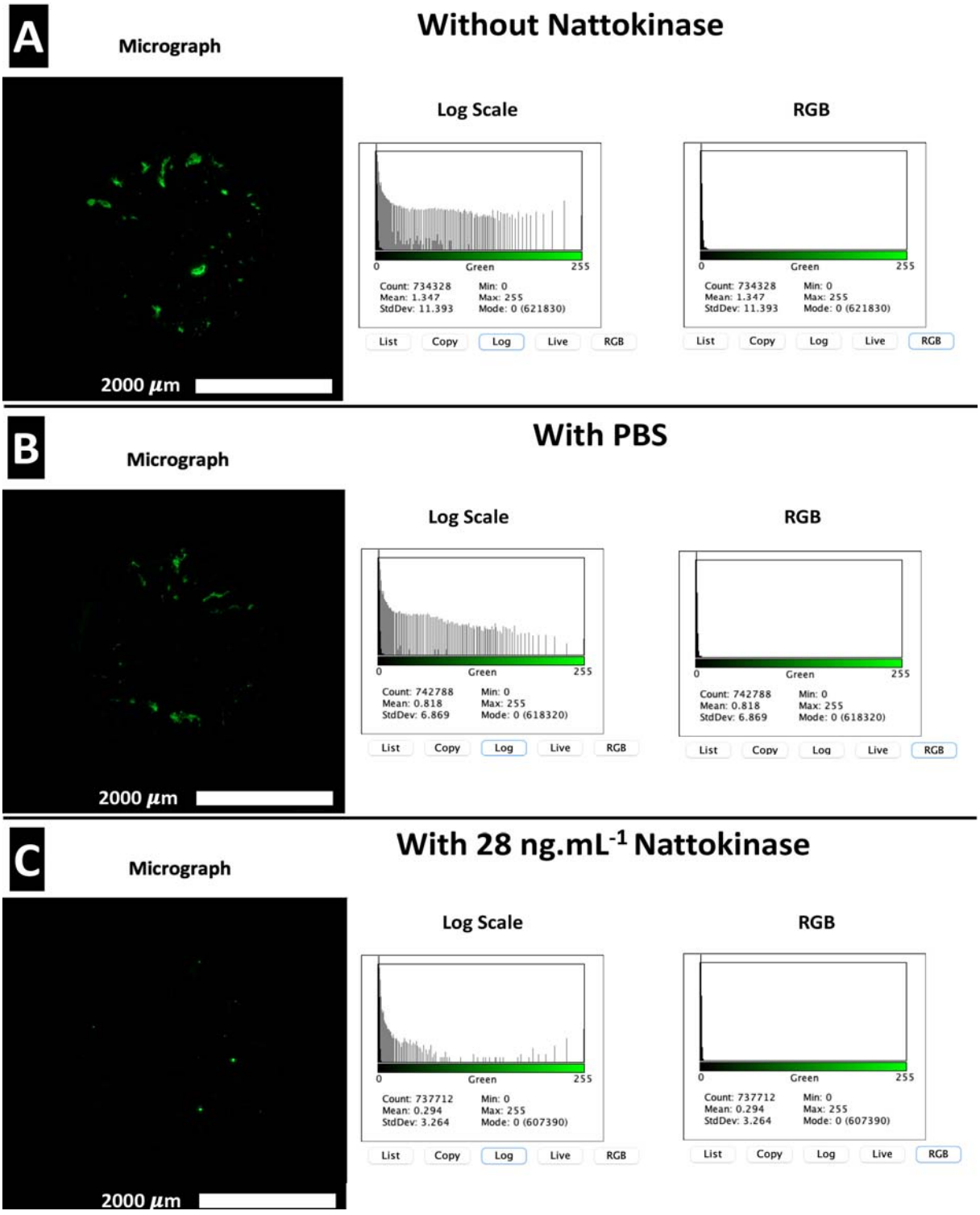

to 28 ng/mL nattokinase

Figure 1. Images of fibrinaloid microclot formation and their removal via nattokinase. Thrombin and fibrinogen were incubated together with thioflavin T and LPS, and imaged after 6h in a Cytation 1, as described in Methods. Further additions were (A) none, (B) PBS, (C) recombinant nattokinase 28 ng/mL. Bar = 2 mm (2,000 µm).

in PBS (Figure 1C, bottom). In addition, the right hand panels of the figure show the 8-bit intensity distributions of pixels on linear and logarithmic scales.

While we sought to avoid any 'cherry picking' in the past, the great attraction of the present approach is that the entire sample is imaged (serially) so this issue is completely avoided. Although not necessarily obvious to the naked eye, there are variations in pixel intensity that allow a thresholding to determine what counts as a clot boundary. Figure 1 also shows the pixel intensity variation for the images displayed on its left side; the logarithmic plot in particular makes clear how much the pixels of larger intensity differed following the addition of the nattokinase.

The time evolution of these data (Figure 2) shows that in the absence of nattokinase the clot numbers increase for an hour or so then decrease slightly before stabilizing (Figure 2A). When nattokinase is present the clot numbers decrease after the first time point and by 2h have attained their lowest level, this being approximately half that of the 14 ng/mL nattokinase (in which the nattokinase level is thus halved), possibly implying a loss of activity over time. In Figure 2B we see the dynamics of the clot intensity (total number of pixels), this being substantially lower in the presence of NK, especially at the higher level of enzyme. Figure 2C shows the time evolution of the median clot size.

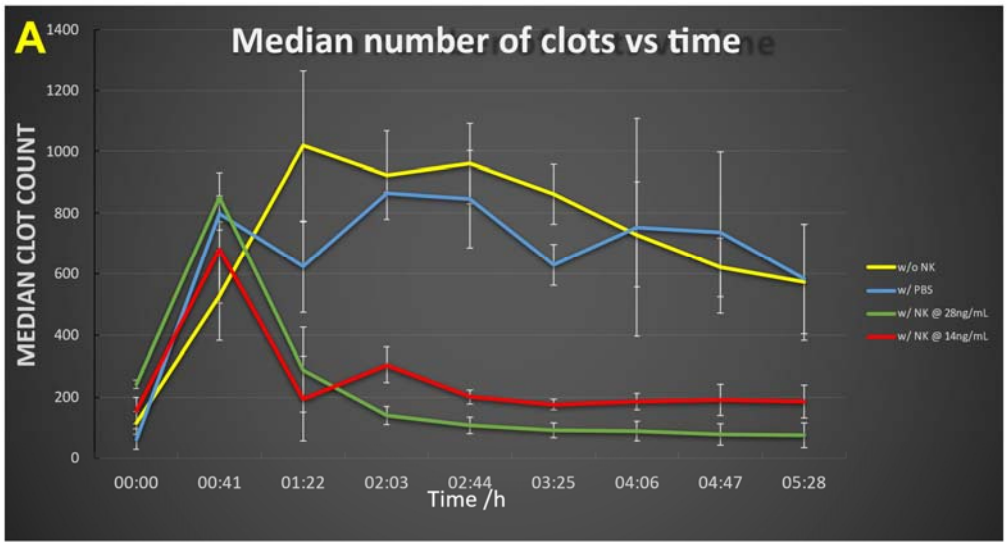

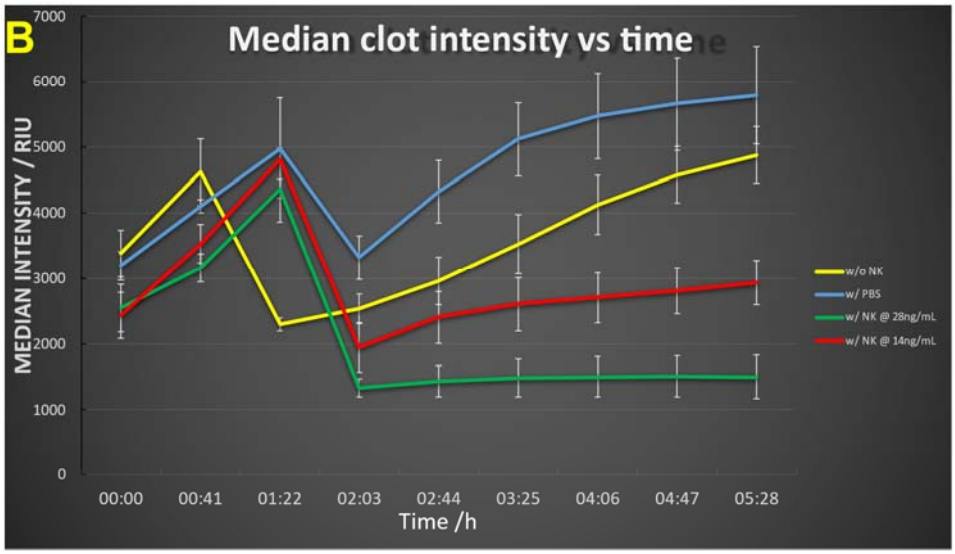

113

114 00

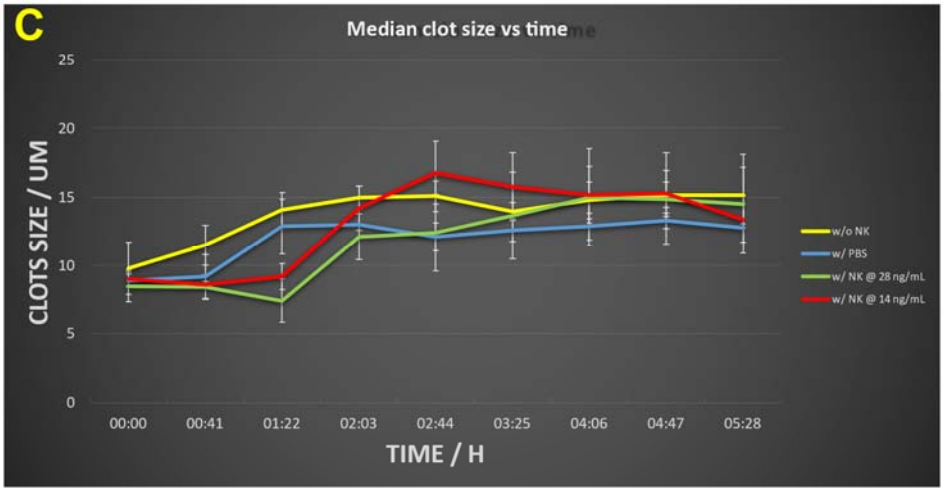

115

116 **Figure 2**. Time evolution of (A) clot number, (B) intensity and (C) median clot size during the development of
117 fibrinaloid microclots and their incubation with nattokinase. Thrombin and fibrinogen were incubated together with
118 thioflavin T, and imaged after 6h in a Cytation 1, as described in Methods. Further additions were none (yellow), PBS

(blue), recombinant nattokinase 28 ng/mL (green), or recombinant nattokinase 14 ng/mL (red). Videos of the incubation with PBS and with nattokinase are given in Supplementary Information.

Three features stand out. First, especially in the absence of NK (yellow trace), the clots increase in number and size over time (Figure 2A, 2B), illustrating how microclots may aggregate to form macroclots, as part of the normal amyloidogenic process (e.g. [173,212,215,239,265-275]). This kind of aggregation may be highly significant in stroke and myocardial infarctions, where clots may be far larger than the simple sloughing off of atherosclerotic plaques might reasonably create. Secondly, the enzyme effectively decreases the rate and extent of microclot formation, in rough proportion to the amount of enzyme (compare e.g. red and green traces at 5h). The lowest intensity point was observed in the interval 2-4h, implying a die-off in activity or instability of the enzyme over time. This is good, in that untrammelled fibrinolytic activity may not be of the greatest therapeutic benefit. Lastly, the median clot size (Fig 2C) increases briefly then stabilizes. This reflects the fact that smaller clots will tend to be degraded preferentially as their surface area per unit mass is significantly greater than that of larger clots. (It is not commonly recognised, but if one imagines two solid spheres, of which one is twice the diameter of the other, the degradation of a given (i.e. the same) mass in the two spheres leads to a loss in mass of just 12.5% of the larger sphere when the smaller one is completely degraded, and a loss in radius of the larger sphere that is less than 5% of its starting value. Consequently, although possibly at first glance surprising, this is, given the traces in Figures 2A and 2B, in fact the result expected for Figure 2C.)

Using Amytracker dyes instead of ThT

Because it is valuable to have other dyes should one wish to use multiple wavelengths (as in [103]), we also assessed the red oligothiophene-class Amytracker™ dyes (Ebba Biotech) (see e.g. [101,103,105,276-283]). However, these gave highly anomalous traces in this system, and we suspect may have inhibited the nattokinase, so were not further pursued.

3. Discussion

The ability to assess the rate of fibrin amyloid formation and degradation noninvasively is highly desirable, as it precisely permits studies of the present type that can then be automated. While still not a high-throughput approach in the usual sense, this does provide a substantial advance in scoring fibrinaloid microclot formation that is both fully quantitative and without undue operator fatigue. This has allowed us, for the first time, to conclude at least three important features: (i) the formation kinetics of fibrin amyloid microclots in whole samples may be imaged noninvasively in an automated manner, (ii) such microclots can aggregate over time, and (iii) the fibrinaloid microclots may be degraded by nattokinase. This latter has significant therapeutic implications for those suffering from Long COVID and related disorders, as NK preparations are widely available commercially. Our approach also thus allows for the comparison of different preparations of NK. Future work could usefully include recombinant serrapeptase (NK/SP), lumbrokinase (NK/LK) and/or sequence variants of NK/SP made using the methods of synthetic biology [284], since both serrapeptase and lumbrokinase also have fibrinolytic and amyloid-degrading properties [60,285-296].

4. Materials and Methods

Assay method

In vitro microclots were made by mixing commercially obtained fibrinogen (Sigma catalogue number 9001-32-5, at a final concentration of 2 mg/mL) and thrombin (Sigma, final amount 14U) with bacterial LPS (Sigma product code L2630-10MG) and used at a final concentration of 1ng / mL and incubated at 37ºC for 30 min. Samples were then exposed to the fluorogenic amyloid dye, Thioflavin T (ThT) (final concentration: 0.03 mM) for 20 mins (protected from light) at room temperature. Following incubation, 10 µL of the recombinantly produced nattokinase at different concentrations / PBS (control) were added. This was then followed by immediately pipetting 15 µL of assay sample onto a 15-well slide 'angiogenesis' glass bottom plate used without a lid (Ibidi: https://ibidi.com/chambered-coverslips/245--slide-15-well-3d-glass-bottom.html), reproduced in Figure 3, and without shaking (cf. [142,297-309]). The excitation wavelength band for ThT was set at 450 nm to 499 nm and the emission at 499 nm to 529 nm. Samples were viewed using Gen5 software on an Agilent BioTek Cytation 1 Cell Imaging Multimode Reader, essentially following the protocol developed and described by Dalton and colleagues [179]. The Cytation instrument is an automated fluorescence microscope with 8-bit intensity resolution in which an entire, large field of view can be constructed at high magnification by taking serial images and moving the stage automatically. With the 4x objective used, each final image (as in Figure 1) was composed of 1296 individual images. The typical file size of a final, stitched .tif image was 19 Mb. Each experiment was run multiple times, each time being in triplicate (three separate wells). Other relevant settings that we optimized for this assay were as follows: the Cytation 1 temperature was set at 37C, and images were taken every 41 minutes for 6 hours. The colour channel used was GFP 469,525 A fixed focal height setting, with a bottom elevation of 549 µm and 0 µm offset was selected. A Z-Stack montage of the entire well was applied, with a step size of 86.9 µm, and 12 slices. Samples were analysed using the Gen5 Image Prime 3.13.15 software supplied with the instrument, and the thresholds for minimum and maximum object (clots) size that could be detected were set at 5 and 500 µm, respectively.

Figure 3. The incubation system used herein, allowing imaging from below

182 **Recombinant nattokinase**

183 Recombinant nattokinase was produced within the Liverpool Gene Mill. The nucleotide sequence for *Bacillus subtilis*
184 nattokinase (Uniprot Q93L66, GenBank: AER52006.1) was synthesised by Twist Bioscience and supplied in the
185 pET28a(+) plasmid. The sequence was modified to include a C-terminal poly-Histidine tag for purification, as well as
186 an N-terminal PelB leader sequence in which the terminal QPAMA residues are replaced by APOIA, and with a
187 penta-aspartate linker for targeting to the periplasmic space [310] plus a ENLYFQ TEV cleavage site and a further SGS
188 linker prior to the nattokinase sequence (beginning AQSVPY). The vector was used to transform chemically compe-
189 tent cells of the Rosetta™ strain of *Escherichia coli* (Novagen) according to the method described by Inoue *et al* [311].
190 Transformed cells were plated on plates of LB-agar (0.5% w/v yeast extract, 1% w/v NaCl, 1% w/v tryptone and 2%
191 agar) supplemented with 50 μg/ml kanamycin and 25 μg/ml chloramphenicol. A single colony from the agar plate
192 was used to inoculate 5 ml of LB broth (0.5% w/v yeast extract, 1% w/v NaCl, 1% w/v tryptone) supplemented with
193 kanamycin and chloramphenicol as described above, for overnight culturing at 37°C with shaking. The culture was
194 diluted to an OD_{600} of 0.05 in 500 ml of LB broth supplemented with kanamycin and chloramphenicol as described
195 above, and incubated with shaking at 37°C. When an OD_{600} of 0.6 was reached, recombinant protein expression was
196 induced by addition of 0.75 mM isopropyl β-D-1-thiogalactopyranoside (IPTG), and the culture was incubated over-
197 night at 18°C with shaking. Cell pellets were harvested by centrifugation at 4000 x*g* for 10 minutes, and the pellets
198 were resuspended in 50 ml of a solution of Tris-HCl (pH8) and 10 mM EDTA, and incubated at 60°C for 2 hours [312].
199 The suspension was centrifuged at 4°C at 16000 x*g* for 10 minutes, and the supernatant was passed through 1 ml of
200 HisPur™ Ni-NTA resin (Thermo Scientific) to purify poly-Histidine-tagged proteins. Bound proteins were eluted us-
201 ing 500 mM imidazole, followed by desalting and concentration using a Pierce™ Protein Concentrator PES (Thermo
202 Scientific) with 30 kDa cut-off. Protein yield was quantified using the Pierce™ Bradford Protein Assay Kit (Thermo
203 Scientific), and samples were frozen with 10% v/v glycerol until further use. Inclusion body formation [313] was not
204 here a significant issue. Figure 4 shows a gel illustrating the final preparation.

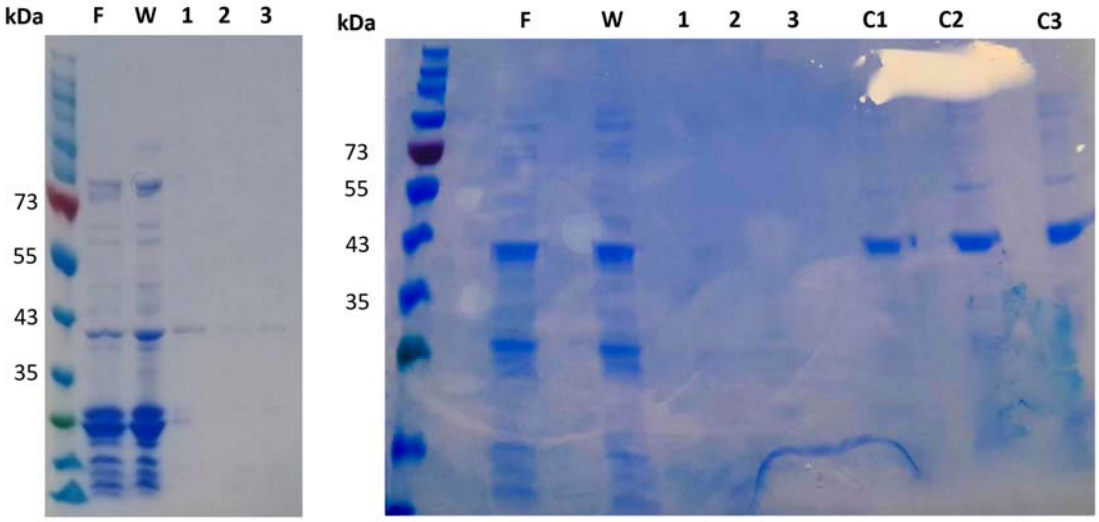

Figure 4: SDS-PAGE of recombinant Nattokinase. F – sample flow-through (unbound proteins); W – fraction of wash buffer (100 mM Tris, pH 7.5, 150 mM NaCl, 50 mM imidazole); 1-3 – purified fractions using elution buffer (100 mM Tris, pH 7.5, 150 mM NaCl, 500 mM imidazole); C1&C2 - purified samples concentrated through 30 kD cut-off protein concentrator unit; C3 - C1 & C2 samples pooled and further concentrated through 3 kD cut-off protein concentrator unit.

205

A kinetic experiment was set up on the Cytation 1 and the effect of nattokinase on microclots was studied at final concentrations of 28 ng/µL and 14 ng/µL, using ThT at a final concentration of 0.005mM, as the fluorogenic dye. Measurements were taken every 40 minutes.

Supplementary figures. Movies (not submitted in preprint) showing a kinetic series of images for samples treated with either PBS (Supplementary Figure 1) or 28 ng/mL nattokinase (Supplementary Figure 2). Frames start from read 1 at time zero and end at read 9 at time 5h 28m. Movies play at 0.5 frames per second. Time zero is the start of the reaction when PBS / NK was added to the sample containing fibrinogen, LPS, Thrombin, and ThT as described in the text. Green annuli are an artefact that may be ignored.

Author Contributions: Conceptualization, DBK & EP; methodology, JMG, JES-S, CWT; resources, DBK & EP.; writing—original draft preparation, DBK; writing—review and editing, All authors; project administration, DBK & EP; funding acquisition DBK & EP. All authors have read and agreed to the published version of the manuscript.

Funding: EP: Funding was provided by NRF of South Africa (grant number 142142) and SA MRC (self-initiated research (SIR) grant), and Balvi Foundation. DBK thanks the Balvi Foundation (grant 18) and the Novo Nordisk Foundation for funding (grant NNF20CC0035580). The content and findings reported and illustrated are the sole deduction, view and responsibility of the researchers and do not reflect the official position and sentiments of the funders.

Acknowledgments: We thank Dr Caroline F. Dalton (Sheffield Hallam University) and Drs Amanda Barnes and Ashley Smith (Agilent) for many helpful discussions about the Cytation system and its optimisation

Conflicts of Interest E.P. is a named inventor on a patent application covering the use of fluorescence methods for microclot detection in Long COVID. The funders had no role in the design of the study; in the collection, analyses, or interpretation of data; in the writing of the manuscript; or in the decision to publish the results.

References

1. Nagareddy, P.; Smyth, S.S. Inflammation and thrombosis in cardiovascular disease. *Curr Opin Hematol* **2013**, *20*, 457-463, doi:10.1097/MOH.0b013e328364219d.
2. Stark, K.; Massberg, S. Interplay between inflammation and thrombosis in cardiovascular pathology. *Nat Rev Cardiol* **2021**, *18*, 666-682, doi:10.1038/s41569-021-00552-1.
3. Wagner, D.D.; Heger, L.A. Thromboinflammation: From Atherosclerosis to COVID-19. *Arterioscler Thromb Vasc Biol* **2022**, *42*, 1103-1112.
4. Kleinbongard, P.; Heusch, G. A fresh look at coronary microembolization. *Nat Rev Cardiol* **2022**, *19*, 265-280, doi:10.1038/s41569-021-00632-2.
5. Lacey, M.J.; Raza, S.; Rehman, H.; Puri, R.; Bhatt, D.L.; Kalra, A. Coronary Embolism: A Systematic Review. *Cardiovasc Revasc Med* **2020**, *21*, 367-374, doi:10.1016/j.carrev.2019.05.012.
6. Nappi, F.; Nappi, P.; Gambardella, I.; Avtaar Singh, S.S. Thromboembolic Disease and Cardiac Thrombotic Complication in COVID-19: A Systematic Review. *Metabolites* **2022**, *12*, 889, doi:10.3390/metabo12100889.

7. Mackman, N.; Bergmeier, W.; Stouffer, G.A.; Weitz, J.I. Therapeutic strategies for thrombosis: new targets and approaches. *Nat Rev Drug Discov* **2020**, *19*, 333-352, doi:10.1038/s41573-020-0061-0.
8. Thakur, M.; Junho, C.V.C.; Bernhard, S.M.; Schindewolf, M.; Noels, H.; Doring, Y. NETs-Induced Thrombosis Impacts on Cardiovascular and Chronic Kidney Disease. *Circ Res* **2023**, *132*, 933-949, doi:10.1161/CIRCRESAHA.123.321750.
9. Lippi, G.; Mattiuzzi, C.; Favaloro, E.J. Novel and emerging therapies: thrombus-targeted fibrinolysis. *Semin Thromb Hemost* **2013**, *39*, 48-58, doi:10.1055/s-0032-1328935.
10. Jackson, S.P.; Darbousset, R.; Schoenwaelder, S.M. Thromboinflammation: challenges of therapeutically targeting coagulation and other host defense mechanisms. *Blood* **2019**, *133*, 906-918, doi:10.1182/blood-2018-11-882993.
11. Medi, C.; Hankey, G.J.; Freedman, S.B. Stroke risk and antithrombotic strategies in atrial fibrillation. *Stroke* **2010**, *41*, 2705-2713, doi:10.1161/STROKEAHA.110.589218.
12. Bikdeli, B.; Madhavan, M.V.; Jimenez, D.; Chuich, T.; Dreyfus, I.; Driggin, E.; Nigoghossian, C.; Ageno, W.; Madjid, M.; Guo, Y.; et al. COVID-19 and Thrombotic or Thromboembolic Disease: Implications for Prevention, Antithrombotic Therapy, and Follow-up. *J Am Coll Cardiol* **2020**, *75*, 2950-2973, doi:10.1016/j.jacc.2020.04.031.
13. Grobler, C.; Maphumulo, S.C.; Grobbelaar, L.M.; Bredenkamp`, J.; Laubscher, J.; Lourens, P.J.; Steenkamp, J.; Kell, D.B.; Pretorius, E. COVID-19: The Rollercoaster of Fibrin(ogen), D-dimer, von Willebrand Factor, P-selectin and Their Interactions with Endothelial Cells, Platelets and Erythrocytes. *Int J Mol Sci* **2020**, *21*, 5168, doi:https://doi.org/10.3390/ijms21145168.
14. Greer, I.A.; Brenner, B.; Gris, J.C. Antithrombotic treatment for pregnancy complications: which path for the journey to precision medicine? *Br J Haematol* **2014**, *165*, 585-599, doi:10.1111/bjh.12813.
15. Undas, A.; Brummel-Ziedins, K.; Mann, K.G. Why does aspirin decrease the risk of venous thromboembolism? On old and novel antithrombotic effects of acetyl salicylic acid. *J Thromb Haemost* **2014**, *12*, 1776-1787, doi:10.1111/jth.12728.
16. Wang, C.; Chen, J.; Tian, W.; Han, Y.; Xu, X.; Ren, T.; Tian, C.; Chen, C. Natto: A medicinal and edible food with health function. *Chin Herb Med* **2023**, *15*, 349-359, doi:10.1016/j.chmed.2023.02.005.
17. Lampe, B.J.; English, J.C. Toxicological assessment of nattokinase derived from *Bacillus subtilis* var. *natto*. *Food Chem Toxicol* **2016**, *88*, 87-99, doi:10.1016/j.fct.2015.12.025.
18. Ruiz Sella, S.R.B.; Bueno, T.; de Oliveira, A.A.B.; Karp, S.G.; Soccol, C.R. *Bacillus subtilis* natto as a potential probiotic in animal nutrition. *Crit Rev Biotechnol* **2021**, *41*, 355-369, doi:10.1080/07388551.2020.1858019.
19. Afzaal, M.; Saeed, F.; Islam, F.; Ateeq, H.; Asghar, A.; Shah, Y.A.; Ofoedu, C.E.; Chacha, J.S. Nutritional Health Perspective of Natto: A Critical Review. *Biochem Res Int* **2022**, *2022*, 5863887, doi:10.1155/2022/5863887.
20. Teramoto, N.; Sato, K.; Wada, T.; Nishikawa, Y.; Kage-Nakadai, E. Impacts of *Bacillus subtilis* var. *natto* on the lifespan and stress resistance of *Caenorhabditis elegans*. *J Appl Microbiol* **2023**, *134*, lxad082, doi:10.1093/jambio/lxad082.
21. Sumi, H.; Hamada, H.; Tsushima, H.; Mihara, H.; Muraki, H. A novel fibrinolytic enzyme (nattokinase) in the vegetable cheese Natto; a typical and popular soybean food in the Japanese diet. *Experientia* **1987**, *43*, 1110-1111, doi:10.1007/BF01956052.
22. Sawamura, S. On the micro-organisms of natto *Bull. Coll. Agric. Tokyo Imperial Univ.* **1906**, *7*, 107-110.
23. Oshima, K. The properties of protease A, the proteolytic enzyme of natto bacteria. *J. Soc. Agric. For. Sapporo* **1925**, *71*, 387-403.
24. Fujita, M.; Hong, K.; Ito, Y.; Misawa, S.; Takeuchi, N.; Kariya, K.; Nishimuro, S. Transport of nattokinase across the rat intestinal tract. *Biol Pharm Bull* **1995**, *18*, 1194-1196, doi:10.1248/bpb.18.1194.
25. Sumi, H.; Hamada, H.; Nakanishi, K.; Hiratani, H. Enhancement of the fibrinolytic activity in plasma by oral administration of nattokinase. *Acta Haematol* **1990**, *84*, 139-143, doi:10.1159/000205051.

26. Sumi, H.; Yanagisawa, Y.; Yatagai, C.; Saito, J. Natto bacillus as an oral fibrinolytic agent: Nattokinase activity and the ingestion effect of *Bacillus subtilis natto*. *Food Science and Technology Research* **2004**, *10*, 17-20.
27. Chen, H.; McGowan, E.M.; Ren, N.; Lal, S.; Nassif, N.; Shad-Kaneez, F.; Qu, X.; Lin, Y. Nattokinase: A Promising Alternative in Prevention and Treatment of Cardiovascular Diseases. *Biomarker Insights* **2018**, *13*, 1177271918785130, doi:10.1177/1177271918785130.
28. Ero, M.P.; Ng, C.M.; Mihailovski, T.; Harvey, N.R.; Lewis, B.H. A pilot study on the serum pharmacokinetics of nattokinase in humans following a single, oral, daily dose. *Altern Ther Health Med* **2013**, *19*, 16-19.
29. Dabbagh, F.; Negahdaripour, M.; Berenjian, A.; Behfar, A.; Mohammadi, F.; Zamani, M.; Irajie, C.; Ghasemi, Y. Nattokinase: production and application. *Appl Microbiol Biotechnol* **2014**, *98*, 9199-9206, doi:10.1007/s00253-014-6135-3.
30. Kapoor, R.; Harde, H.; Jain, S.; Panda, A.K.; Panda, B.P. Downstream Processing, Formulation Development and Antithrombotic Evaluation of Microbial Nattokinase. *J Biomed Nanotechnol* **2015**, *11*, 1213-1224, doi:10.1166/jbn.2015.2071.
31. Zhou, X.Q.; Liu, L.Z.; Zeng, X.R. Research progress on the utilisation of embedding technology and suitable delivery systems for improving the bioavailability of nattokinase: A review. *Food Structure-Netherlands* **2021**, *30*.
32. Liu, S.; Zhu, J.; Liu, C.; Li, J.; Li, Z.; Zhao, J.; Liu, H. Synthesis of sustained release/controlled release nanoparticles carrying nattokinase and their application in thrombolysis. *Pharmazie* **2021**, *76*, 145-149, doi:10.1691/ph.2021.0155.
33. Priya, V.; Samridhi; Singh, N.; Dash, D.; Muthu, M.S. Nattokinase Encapsulated Nanomedicine for Targeted Thrombolysis: Development, Improved in Vivo Thrombolytic Effects, and Ultrasound/Photoacoustic Imaging. *Mol Pharm* **2024**, *21*, 283-302, doi:10.1021/acs.molpharmaceut.3c00830.
34. Wei, X.; Luo, M.; Xie, Y.; Yang, L.; Li, H.; Xu, L.; Liu, H. Strain screening, fermentation, separation, and encapsulation for production of nattokinase functional food. *Appl Biochem Biotechnol* **2012**, *168*, 1753-1764, doi:10.1007/s12010-012-9894-2.
35. Peng, Y.; Yang, X.; Zhang, Y. Microbial fibrinolytic enzymes: an overview of source, production, properties, and thrombolytic activity in vivo. *Appl Microbiol Biotechnol* **2005**, *69*, 126-132, doi:10.1007/s00253-005-0159-7.
36. Li, D.; Hou, L.; Hu, M.; Gao, Y.; Tian, Z.; Fan, B.; Li, S.; Wang, F. Recent Advances in Nattokinase-Enriched Fermented Soybean Foods: A Review. *Foods* **2022**, *11*, 1867, doi:10.3390/foods11131867.
37. Kurosawa, Y.; Nirengi, S.; Homma, T.; Esaki, K.; Ohta, M.; Clark, J.F.; Hamaoka, T. A single-dose of oral nattokinase potentiates thrombolysis and anti-coagulation profiles. *Sci Rep* **2015**, *5*, 11601, doi:10.1038/srep11601.
38. Selvarajan, E.; Bhatnagar, N. Nattokinase: an updated critical review on challenges and perspectives. *Cardiovasc Hematol Agents Med Chem* **2017**, *15*, 126-135, doi:10.2174/1871525716666171207153332.
39. Weng, Y.; Yao, J.; Sparks, S.; Wang, K.Y. Nattokinase: An Oral Antithrombotic Agent for the Prevention of Cardiovascular Disease. *Int J Mol Sci* **2017**, *18*, 523, doi:10.3390/ijms18030523.
40. Derosa, G.; Maffioli, P.; D'Angelo, A.; Di Pierro, F. Nutraceutical Approach to Preventing Coronavirus Disease 2019 and Related Complications. *Front Immunol* **2021**, *12*, 582556, doi:10.3389/fimmu.2021.582556.
41. Takagaki, S.; Suzuki, M.; Suzuki, E.; Hasumi, K. Unsaturated fatty acids enhance the fibrinolytic activity of subtilisin NAT (nattokinase). *J Food Biochem* **2020**, *44*, e13326, doi:10.1111/jfbc.13326.
42. Li, X.M.; Long, J.Z.; Gao, Q.; Pan, M.Y.; Wang, J.; Yang, F.J.; Zhang, Y. Nattokinase Supplementation and Cardiovascular Risk Factors: A Systematic Review and Meta-Analysis of Randomized Controlled Trials. *Rev Cardiovasc Med* **2023**, *24*, 234, doi:https://doi.org/10.31083/j.rcm2408234.
43. Jamali, N.; Vahedi, F.; Fard, E.S.; Taheri-Anganehd, M.; Taghvimi, S.; Khatami, S.H.; Ghasemi, H.; Movahedpour, A. Nattokinase: Structure, applications and sources. *Biocatal Agric Biotechnolo* **2023**, *47*, 102564, doi:https://doi.org/10.1016/j.bcab.2022.102564.
44. Yuan, L.; Liangqi, C.; Xiyu, T.; Jinyao, L. Biotechnology, Bioengineering and Applications of *Bacillus* Nattokinase. *Biomolecules* **2022**, *12*, 980, doi:10.3390/biom12070980.

45. Nara, N.; Kurosawa, Y.; Fuse-Hamaoka, S.; Kuroiwa, M.; Endo, T.; Tanaka, R.; Kime, R.; Hamaoka, T. A single dose of oral nattokinase accelerates skin temperature recovery after cold water immersion: A double-blind, placebo-controlled crossover study. *Heliyon* **2023**, *9*, e17951, doi:10.1016/j.heliyon.2023.e17951.
46. Di Micco, P.; Bernardi, F.F.; Camporese, G.; Biglietto, M.; Perrella, A.; Ciarambino, T.; Russo, V.; Imbalzano, E. Nattokinase historical sketch on experimental and clinical evidence *Ital J Med* **2023**, *17*, 1583, doi:10.4081/itjm.2023.1583
47. Kawamata, T.; Wakimoto, A.; Nishikawa, T.; Ikezawa, M.; Hamada, M.; Inoue, Y.; Kulathunga, K.; Salim, F.N.; Kanai, M.; Nishino, T.; et al. Natto consumption suppresses atherosclerotic plaque progression in LDL receptor-deficient mice transplanted with iRFP-expressing hematopoietic cells. *Sci Rep* **2023**, *13*, 22469, doi:10.1038/s41598-023-48562-y.
48. Sun, R.; Li, D.; Sun, M.; Miao, X.; Jin, X.; Xu, X.; Su, Y.; Xu, H.; Wang, J.; Niu, H. *Bacillus* natto ameliorates obesity by regulating PI3K/AKT pathways in rats. *Biochem Biophys Res Commun* **2022**, *603*, 160-166, doi:10.1016/j.bbrc.2022.03.012.
49. Ibe, S.; Kumada, K.; Yoshida, K.; Otobe, K. Natto (fermented soybean) extract extends the adult lifespan of *Caenorhabditis elegans*. *Biosci Biotechnol Biochem* **2013**, *77*, 392-394, doi:10.1271/bbb.120726.
50. Guilherme do Prado, F.; Pagnoncelli, M.G.B.; de Melo Pereira, G.V.; Karp, S.G.; Soccol, C.R. Fermented Soy Products and Their Potential Health Benefits: A Review. *Microorganisms* **2022**, *10*, 1606, doi:10.3390/microorganisms10081606.
51. Yatagai, C.; Maruyama, M.; Kawahara, T.; Sumi, H. Nattokinase-promoted tissue plasminogen activator release from human cells. *Pathophysiol Haemost Thromb* **2008**, *36*, 227-232, doi:10.1159/000252817.
52. Takabayashi, T.; Imoto, Y.; Sakashita, M.; Kato, Y.; Tokunaga, T.; Yoshida, K.; Narita, N.; Ishizuka, T.; Fujieda, S. Nattokinase, profibrinolytic enzyme, effectively shrinks the nasal polyp tissue and decreases viscosity of mucus. *Allergol Int* **2017**, *66*, 594-602, doi:10.1016/j.alit.2017.03.007.
53. Hsia, C.H.; Shen, M.C.; Lin, J.S.; Wen, Y.K.; Hwang, K.L.; Cham, T.M.; Yang, N.C. Nattokinase decreases plasma levels of fibrinogen, factor VII, and factor VIII in human subjects. *Nutr Res* **2009**, *29*, 190-196, doi:10.1016/j.nutres.2009.01.009.
54. Wang, P.; Peng, C.; Xie, X.; Deng, X.; Weng, M. Research progress on the fibrinolytic enzymes produced from traditional fermented foods. *Food Sci Nutr* **2023**, *11*, 5675-5688, doi:10.1002/fsn3.3601.
55. Kumar, S.S.; Sabu, A. Fibrinolytic Enzymes for Thrombolytic Therapy. *Adv Exp Med Biol* **2019**, *1148*, 345-381, doi:10.1007/978-981-13-7709-9_15.
56. Fang, M.; Yuan, B.; Wang, M.; Liu, J.; Wang, Z. Nattokinase: Insights into Biological Activity, Therapeutic Applications, and the Influence of Microbial Fermentation. *Fermentation* **2023**, *9*, 950, doi:https://doi.org/10.3390/fermentation9110950.
57. Hazare, C.; Bhagwat, P.; Singh, S.; Pillai, S. Diverse origins of fibrinolytic enzymes: A comprehensive review. *Heliyon* **2024**, *10*, e26668, doi:10.1016/j.heliyon.2024.e26668.
58. Diwan, D.; Usmani, Z.; Sharma, M.; Nelson, J.W.; Thakur, V.K.; Christie, G.; Molina, G.; Gupta, V.K. Thrombolytic Enzymes of Microbial Origin: A Review. *Int J Mol Sci* **2021**, *22*, 10468.
59. Kotb, E. Activity assessment of microbial fibrinolytic enzymes. *Appl Microbiol Biotechnol* **2013**, *97*, 6647-6665, doi:10.1007/s00253-013-5052-1.
60. Mousavi Ghahfarrokhi, S.S.; Mahdigholi, F.S.; Amin, M. Collateral beauty in the damages: an overview of cosmetics and therapeutic applications of microbial proteases. *Arch Microbiol* **2023**, *205*, 375, doi:10.1007/s00203-023-03713-7.
61. Wu, H.; Wang, H.; Xu, F.; Chen, J.; Duan, L.; Zhang, F. Acute toxicity and genotoxicity evaluations of Nattokinase, a promising agent for cardiovascular diseases prevention. *Regul Toxicol Pharmacol* **2019**, *103*, 205-209, doi:10.1016/j.yrtph.2019.02.006.
62. Gallelli, G.; Di Mizio, G.; Palleria, C.; Siniscalchi, A.; Rubino, P.; Muraca, L.; Cione, E.; Salerno, M.; De Sarro, G.; Gallelli, L. Data Recorded in Real Life Support the Safety of Nattokinase in Patients with Vascular Diseases. *Nutrients* **2021**, *13*, 2031, doi:10.3390/nu13062031.

63. Bresson, J.-L.; Burlingame, B.; Dean, T.; Fairweather-Tait, S.; Heinonen, M.; Hirsch-Ernst, K.I.; Mangelsdorf, I.; McArdle, H.; Naska, A.; Neuhäuser-Berthold, M.; et al. Safety of fermented soybean extract NSK-SD®as anovel food pursuant to Regulation (EC) No 258/97. *EFSA J* **2016**, *14*, 4541, doi:10.2903/j.efsa.2016.4541.
64. Yanagisawa, Y.; Chatake, T.; Chiba-Kamoshida, K.; Naito, S.; Ohsugi, T.; Sumi, H.; Yasuda, I.; Morimoto, Y. Purification, crystallization and preliminary X-ray diffraction experiment of nattokinase from *Bacillus subtilis* natto. *Acta Crystallogr Sect F Struct Biol Cryst Commun* **2010**, *66*, 1670-1673, doi:10.1107/S1744309110043137.
65. Yanagisawa, Y.; Chatake, T.; Naito, S.; Ohsugi, T.; Yatagai, C.; Sumi, H.; Kawaguchi, A.; Chiba-Kamosida, K.; Ogawa, M.; Adachi, T.; et al. X-ray structure determination and deuteration of nattokinase. *J Synchrotron Radiat* **2013**, *20*, 875-879, doi:10.1107/S0909049513020700.
66. Minh, N.H.; Trang, H.T.Q.; Van, T.B.; Loc, N.H. Production and purification of nattokinase from *Bacillus subtilis*. *Food Biotechnology* **2022**, *36*, 1-21.
67. Wang, C.; Du, M.; Zheng, D.; Kong, F.; Zu, G.; Feng, Y. Purification and characterization of nattokinase from *Bacillus subtilis* natto B-12. *J Agric Food Chem* **2009**, *57*, 9722-9729, doi:10.1021/jf901861v.
68. Fujita, M.; Nomura, K.; Hong, K.; Ito, Y.; Asada, A.; Nishimuro, S. Purification and characterization of a strong fibrinolytic enzyme (nattokinase) in the vegetable cheese natto, a popular soybean fermented food in Japan. *Biochem Biophys Res Commun* **1993**, *197*, 1340-1347, doi:10.1006/bbrc.1993.2624.
69. Yin, L.J.; Lin, H.H.; Jiang, S.T. Bioproperties of potent nattokinase from *Bacillus subtilis* YJ1. *J Agric Food Chem* **2010**, *58*, 5737-5742, doi:10.1021/jf100290h.
70. Pagnoncelli, M.G.B.; Fernandes, M.J.; Rodrigues, C.; Soccol, C.R. Nattokinases. In *Current Developments in Biotechnology and Bioengineering: Production, Isolation and Purification of Industrial Products*, Pandey, A., Negi, S., Soccol, C.R., Eds.; Elsevier: Amsterdam, 2017; pp. 509-526.
71. Modi, A.; Raval, I.; Doshi, P.; Joshi, M.; Joshi, C.; Patel, A.K. Heterologous expression of recombinant nattokinase in *Escherichia coli* BL21(DE3) and media optimization for overproduction of nattokinase using RSM. *Protein Expr Purif* **2023**, *203*, 106198, doi:10.1016/j.pep.2022.106198.
72. Ni, H.; Guo, P.C.; Jiang, W.L.; Fan, X.M.; Luo, X.Y.; Li, H.H. Expression of nattokinase in *Escherichia coli* and renaturation of its inclusion body. *J Biotechnol* **2016**, *231*, 65-71, doi:10.1016/j.jbiotec.2016.05.034.
73. Liang, X.; Jia, S.; Sun, Y.; Chen, M.; Chen, X.; Zhong, J.; Huan, L. Secretory expression of nattokinase from *Bacillus subtilis* YF38 in *Escherichia coli*. *Mol Biotechnol* **2007**, *37*, 187-194, doi:10.1007/s12033-007-0060-y.
74. Liang, X.; Zhang, L.; Zhong, J.; Huan, L. Secretory expression of a heterologous nattokinase in *Lactococcus lactis*. *Appl Microbiol Biotechnol* **2007**, *75*, 95-101, doi:10.1007/s00253-006-0809-4.
75. Chen, P.T.; Chiang, C.J.; Chao, Y.P. Medium optimization for the production of recombinant nattokinase by *Bacillus subtilis* using response surface methodology. *Biotechnol Prog* **2007**, *23*, 1327-1332, doi:10.1021/bp070109b.
76. Chen, P.T.; Chiang, C.J.; Chao, Y.P. Strategy to approach stable production of recombinant nattokinase in *Bacillus subtilis*. *Biotechnol Prog* **2007**, *23*, 808-813, doi:10.1021/bp070108j.
77. Cai, D.; Zhu, C.; Chen, S. Microbial production of nattokinase: current progress, challenge and prospect. *World J Microbiol Biotechnol* **2017**, *33*, 84, doi:10.1007/s11274-017-2253-2.
78. Liu, Z.; Zheng, W.; Ge, C.; Cui, W.; Zhou, L.; Zhou, Z. High-level extracellular production of recombinant nattokinase in Bacillus subtilis WB800 by multiple tandem promoters. *BMC Microbiol* **2019**, *19*, 89, doi:10.1186/s12866-019-1461-3.
79. Liu, Z.; Zhao, H.; Han, L.; Cui, W.; Zhou, L.; Zhou, Z. Improvement of the acid resistance, catalytic efficiency, and thermostability of nattokinase by multisite-directed mutagenesis. *Biotechnol Bioeng* **2019**, *116*, 1833-1843, doi:10.1002/bit.26983.

80. Li, C.; Du, Z.; Qi, S.; Zhang, X.; Wang, M.; Zhou, Y.; Lu, H.; Gu, X.; Tian, H. Food-grade expression of nattokinase in *Lactobacillus delbrueckii* subsp. *bulgaricus* and its thrombolytic activity in vitro. *Biotechnol Lett* **2020**, *42*, 2179-2187, doi:10.1007/s10529-020-02974-2.
81. Wei, X.; Zhou, Y.; Chen, J.; Cai, D.; Wang, D.; Qi, G.; Chen, S. Efficient expression of nattokinase in *Bacillus licheniformis*: host strain construction and signal peptide optimization. *J Ind Microbiol Biotechnol* **2015**, *42*, 287-295, doi:10.1007/s10295-014-1559-4.
82. Guangbo, Y.; Min, S.; Wei, S.; Lixin, M.; Chao, Z.; Yaping, W.; Zunxi, H. Heterologous expression of nattokinase from *B. subtilis natto* using *Pichia pastoris* GS115 and assessment of its thrombolytic activity. *BMC Biotechnol* **2021**, *21*, 49, doi:10.1186/s12896-021-00708-4.
83. Sheng, Y.; Yang, J.; Wang, C.; Sun, X.; Yan, L. Microbial nattokinase: from synthesis to potential application. *Food Funct* **2023**, *14*, 2568-2585, doi:10.1039/d2fo03389e.
84. Urano, T.; Ihara, H.; Umemura, K.; Suzuki, Y.; Oike, M.; Akita, S.; Tsukamoto, Y.; Suzuki, I.; Takada, A. The profibrinolytic enzyme subtilisin NAT purified from *Bacillus subtilis* cleaves and inactivates plasminogen activator inhibitor type 1. *J Biol Chem* **2001**, *276*, 24690-24696, doi:10.1074/jbc.M101751200.
85. Jang, J.Y.; Kim, T.S.; Cai, J.; Kim, J.; Kim, Y.; Shin, K.; Kim, K.S.; Park, S.K.; Lee, S.P.; Choi, E.K.; et al. Nattokinase improves blood flow by inhibiting platelet aggregation and thrombus formation. *Lab Anim Res* **2013**, *29*, 221-225, doi:10.5625/lar.2013.29.4.221.
86. Wu, H.; Wang, Y.; Zhang, Y.; Xu, F.; Chen, J.; Duan, L.; Zhang, T.; Wang, J.; Zhang, F. Breaking the vicious loop between inflammation, oxidative stress and coagulation, a novel anti-thrombus insight of nattokinase by inhibiting LPS-induced inflammation and oxidative stress. *Redox Biol* **2020**, *32*, 101500, doi:10.1016/j.redox.2020.101500.
87. Fujita, M.; Ohnishi, K.; Takaoka, S.; Ogasawara, K.; Fukuyama, R.; Nakamuta, H. Antihypertensive effects of continuous oral administration of nattokinase and its fragments in spontaneously hypertensive rats. *Biol Pharm Bull* **2011**, *34*, 1696-1701, doi:10.1248/bpb.34.1696.
88. Kim, J.Y.; Gum, S.N.; Paik, J.K.; Lim, H.H.; Kim, K.C.; Ogasawara, K.; Inoue, K.; Park, S.; Jang, Y.; Lee, J.H. Effects of nattokinase on blood pressure: a randomized, controlled trial. *Hypertens Res* **2008**, *31*, 1583-1588, doi:10.1291/hypres.31.1583.
89. Jensen, G.S.; Lenninger, M.; Ero, M.P.; Benson, K.F. Consumption of nattokinase is associated with reduced blood pressure and von Willebrand factor, a cardiovascular risk marker: results from a randomized, double-blind, placebo-controlled, multicenter North American clinical trial. *Integr Blood Press Control* **2016**, *9*, 95-104, doi:10.2147/IBPC.S99553.
90. Elbakry, M.M.M.; Mansour, S.Z.; Helal, H.; Ahmed, E.S.A. Nattokinase attenuates bisphenol A or gamma irradiation-mediated hepatic and neural toxicity by activation of Nrf2 and suppression of inflammatory mediators in rats. *Environ Sci Pollut Res Int* **2022**, *29*, 75086-75100, doi:10.1007/s11356-022-21126-9.
91. Maslarov, D.; Drenska, D.; Maslarova-Gelov, J.; Gelov, I. Understanding the concept of Nattokinase use: a few years after beginning. *Biotechnol Biotechnol Equip* **2023**, *37*, 2249552, doi:https://doi.org/10.1080/13102818.2023.2249552.
92. Chen, H.; Chen, J.; Zhang, F.; Li, Y.; Wang, R.; Zheng, Q.; Zhang, X.; Zeng, J.; Xu, F.; Lin, Y. Effective management of atherosclerosis progress and hyperlipidemia with nattokinase: A clinical study with 1,062 participants. *Front Cardiovasc Med* **2022**, *9*, 964977, doi:10.3389/fcvm.2022.964977.
93. Pretorius, E.; Swanepoel, A.C.; Oberholzer, H.M.; van der Spuy, W.J.; Duim, W.; Wessels, P.F. A descriptive investigation of the ultrastructure of fibrin networks in thrombo-embolic ischemic stroke. *J Thromb Thrombolysis* **2011**, *31*, 507-513, doi:10.1007/s11239-010-0538-5.
94. Pretorius, E. The use of a desktop scanning electron microscope as a diagnostic tool in studying fibrin networks of thrombo-embolic ischemic stroke. *Ultrastruct Pathol* **2011**, *35*, 245-250, doi:10.3109/01913123.2011.606659.

95. Pretorius, E.; Oberholzer, H.M.; van der Spuy, W.J.; Swanepoel, A.C.; Soma, P. Qualitative scanning electron microscopy analysis of fibrin networks and platelet abnormalities in diabetes. *Blood Coagul Fibrinol* **2011**, *22*, 463-467, doi:10.1097/MBC.0b013e3283468a0d.
96. Pretorius, E.; Vermeulen, N.; Bester, J.; Lipinski, B.; Kell, D.B. A novel method for assessing the role of iron and its functional chelation in fibrin fibril formation: the use of scanning electron microscopy. *Toxicol Mech Methods* **2013**, *23*, 352-359, doi:10.3109/15376516.2012.762082.
97. Pretorius, E.; Mbotwe, S.; Bester, J.; Robinson, C.J.; Kell, D.B. Acute induction of anomalous and amyloidogenic blood clotting by molecular amplification of highly substoichiometric levels of bacterial lipopolysaccharide. *J R Soc Interface* **2016**, *123*, 20160539, doi:http://dx.doi.org/10.1098/rsif.2016.0539.
98. Kell, D.B.; Pretorius, E. Proteins behaving badly. Substoichiometric molecular control and amplification of the initiation and nature of amyloid fibril formation: lessons from and for blood clotting. *Progr Biophys Mol Biol* **2017**, *123*, 16-41, doi:DOI http://dx.doi.org/10.1016/j.pbiomolbio.2016.08.006.
99. Pretorius, E.; Mbotwe, S.; Kell, D.B. Lipopolysaccharide-binding protein (LBP) reverses the amyloid state of fibrin seen in plasma of type 2 diabetics with cardiovascular comorbidities. *Sci Rep* **2017**, *7*, 9680.
100. Pretorius, E.; Page, M.J.; Hendricks, L.; Nkosi, N.B.; Benson, S.R.; Kell, D.B. Both lipopolysaccharide and lipoteichoic acids potently induce anomalous fibrin amyloid formation: assessment with novel Amytracker™ stains. bioRxiv preprint. *bioRxiv* **2017**, 143867.
101. Pretorius, E.; Page, M.J.; Engelbrecht, L.; Ellis, G.C.; Kell, D.B. Substantial fibrin amyloidogenesis in type 2 diabetes assessed using amyloid-selective fluorescent stains. *Cardiovasc Diabetol* **2017**, *16*, 141, doi:https://doi.org/10.1186/s12933-017-0624-5.
102. Pretorius, E.; Page, M.J.; Mbotwe, S.; Kell, D.B. Lipopolysaccharide-binding protein (LBP) can reverse the amyloid state of fibrin seen or induced in Parkinson's disease. *PlosOne* **2018**, *13*, e0192121, doi:https://doi.org/10.1371/journal.pone.0192121.
103. Pretorius, E.; Page, M.J.; Hendricks, L.; Nkosi, N.B.; Benson, S.R.; Kell, D.B. Both lipopolysaccharide and lipoteichoic acids potently induce anomalous fibrin amyloid formation: assessment with novel Amytracker™ stains. *J R Soc Interface* **2018**, *15*, 20170941.
104. Pretorius, E.; Bester, J.; Page, M.J.; Kell, D.B. The potential of LPS-binding protein to reverse amyloid formation in plasma fibrin of individuals with Alzheimer-type dementia. *Frontiers Aging Neurosci* **2018**, *10*, 257, doi:doi: 10.3389/fnagi.2018.00257
105. de Waal, G.M.; Engelbrecht, L.; Davis, T.; de Villiers, W.J.S.; Kell, D.B.; Pretorius, E. Correlative Light-Electron Microscopy detects lipopolysaccharide and its association with fibrin fibres in Parkinson's Disease, Alzheimer's Disease and Type 2 Diabetes Mellitus. *Sci Rep* **2018**, *8*, 16798, doi:10.1038/s41598-018-35009-y.
106. Pretorius, E.; Venter, C.; Laubscher, G.J.; Kotze, M.J.; Oladejo, S.; Watson, L.R.; Rajaratnam, K.; Watson, B.W.; Kell, D.B. Prevalence of symptoms, comorbidities, fibrin amyloid microclots and platelet pathology in individuals with Long COVID/ Post-Acute Sequelae of COVID-19 (PASC) *Cardiovasc Diabetol* **2022**, *21*, 148, doi:https://doi.org/10.1186/s12933-022-01579-5.
107. Kell, D.B.; Pretorius, E. Are fibrinaloid microclots a cause of autoimmunity in Long Covid and other post-infection diseases? *Biochem J* **2023**, *480*, 1217-1240, doi:https://doi.org/10.1042/BCJ20230241.
108. Candelise, N.; Baiardi, S.; Franceschini, A.; Rossi, M.; Parchi, P. Towards an improved early diagnosis of neurodegenerative diseases: the emerging role of in vitro conversion assays for protein amyloids. *Acta Neuropathol Commun* **2020**, *8*, 117, doi:10.1186/s40478-020-00990-x.
109. Poleggi, A.; Baiardi, S.; Ladogana, A.; Parchi, P. The Use of Real-Time Quaking-Induced Conversion for the Diagnosis of Human Prion Diseases. *Front Aging Neurosci* **2022**, *14*, 874734, doi:10.3389/fnagi.2022.874734.

110. Grobbelaar, L.M.; Venter, C.; Vlok, M.; Ngoepe, M.; Laubscher, G.J.; Lourens, P.J.; Steenkamp, J.; Kell, D.B.; Pretorius, E. SARS-CoV-2 spike protein S1 induces fibrin(ogen) resistant to fibrinolysis: implications for microclot formation in COVID-19. *Biosci Rep* **2021**, *41*, BSR20210611, doi:10.1042/BSR20210611.
111. Kell, D.B.; Pretorius, E. The simultaneous occurrence of both hypercoagulability and hypofibrinolysis in blood and serum during systemic inflammation, and the roles of iron and fibrin(ogen). *Integr Biol* **2015**, *7*, 24-52, doi:10.1039/c4ib00173g.
112. Bergaglio, T.; Synhaivska, O.; Nirmalraj, P.N. 3D Holo-tomographic Mapping of COVID-19 Microclots in Blood to Assess Disease Severity. *ACS Chem Biomed Imaging* **2024**, online, doi:10.1101/2023.09.12.557318.
113. Stewart, K.L.; Radford, S.E. Amyloid plaques beyond Abeta: a survey of the diverse modulators of amyloid aggregation. *Biophys Rev* **2017**, *9*, 405-419, doi:10.1007/s12551-017-0271-9.
114. Gligorijević, N.; Simeon, M.; Mirjana, R.; Steva, L.; Milan, N.; Tanja, Ć.V.; Olgica, N. Ligand binding to fibrinogen influences its structure and function. *Biol Serb* **2021**, *43*, 24-31, doi:10.5281/zenodo.5512285.
115. Gligorijević, N.; Vasović, T.; Lević, S.; Miljević, Č.; Nedić, O.; Nikolić, M. Atypical antipsychotic clozapine binds fibrinogen and affects fibrin formation. *Int J Biol Macromol* **2020**, *154*, 142-149, doi:10.1016/j.ijbiomac.2020.03.119.
116. Liu, B.; Moloney, A.; Meehan, S.; Morris, K.; Thomas, S.E.; Serpell, L.C.; Hider, R.; Marciniak, S.J.; Lomas, D.A.; Crowther, D.C. Iron promotes the toxicity of amyloid beta peptide by impeding its ordered aggregation. *J Biol Chem* **2011**, *286*, 4248-4256.
117. Louros, N.; Schymkowitz, J.; Rousseau, F. Mechanisms and pathology of protein misfolding and aggregation. *Nat Rev Mol Cell Biol* **2023**, *24*, 912-933, doi:10.1038/s41580-023-00647-2.
118. Xu, Y.; Maya-Martinez, R.; Guthertz, N.; Heath, G.R.; Manfield, I.W.; Breeze, A.L.; Sobott, F.; Foster, R.; Radford, S.E. Tuning the rate of aggregation of hIAPP into amyloid using small-molecule modulators of assembly. *Nat Commun* **2022**, *13*, 1040, doi:10.1038/s41467-022-28660-7.
119. Heller, G.T.; Aprile, F.A.; Michaels, T.C.T.; Limbocker, R.; Perni, M.; Ruggeri, F.S.; Mannini, B.; Lohr, T.; Bonomi, M.; Camilloni, C.; et al. Small-molecule sequestration of amyloid-beta as a drug discovery strategy for Alzheimer's disease. *Sci Adv* **2020**, *6*, eabb5924, doi:10.1126/sciadv.abb5924.
120. Ziaunys, M.; Sneideris, T.; Smirnovas, V. Formation of distinct prion protein amyloid fibrils under identical experimental conditions. *Sci Rep* **2020**, *10*, 4572, doi:10.1038/s41598-020-61663-2.
121. Ziaunys, M.; Sakalauskas, A.; Mikalauskaite, K.; Snieckute, R.; Smirnovas, V. Temperature-Dependent Structural Variability of Prion Protein Amyloid Fibrils. *Int J Mol Sci* **2021**, *22*, 5075, doi:10.3390/ijms22105075.
122. Watts, J.C.; Condello, C.; Stohr, J.; Oehler, A.; Lee, J.; DeArmond, S.J.; Lannfelt, L.; Ingelsson, M.; Giles, K.; Prusiner, S.B. Serial propagation of distinct strains of Abeta prions from Alzheimer's disease patients. *Proc Natl Acad Sci* **2014**, *111*, 10323-10328, doi:10.1073/pnas.1408900111.
123. Han, Z.Z.; Kang, S.G.; Arce, L.; Westaway, D. Prion-like strain effects in tauopathies. *Cell Tissue Res* **2022**, 1-21, doi:10.1007/s00441-022-03620-1.
124. Shoup, D.; Priola, S.A. Cell biology of prion strains in vivo and in vitro. *Cell Tissue Res* **2022**, doi:10.1007/s00441-021-03572-y.
125. Bartz, J.C. Prion Strain Diversity. *Cold Spring Harb Perspect Med* **2016**, *6*, doi:10.1101/cshperspect.a024349.
126. Igel-Egalon, A.; Béringue, V.; Rezaei, H.; Sibille, P. Prion Strains and Transmission Barrier Phenomena. *Pathogens* **2018**, *7*, 5, doi:10.3390/pathogens7010005.
127. Scialò, C.; De Cecco, E.; Manganotti, P.; Legname, G. Prion and Prion-Like Protein Strains: Deciphering the Molecular Basis of Heterogeneity in Neurodegeneration. *Viruses* **2019**, *11*, 261, doi:10.3390/v11030261.
128. Levavasseur, E.; Privat, N.; Haïk, S. *In vitro* Modeling of Prion Strain Tropism. *Viruses* **2019**, *11*, 236, doi:10.3390/v11030236.

129. Peden, A.H.; Suleiman, S.; Barria, M.A. Understanding Intra-Species and Inter-Species Prion Conversion and Zoonotic Potential Using Protein Misfolding Cyclic Amplification. *Front Aging Neurosci* **2021**, *13*, 716452, doi:10.3389/fnagi.2021.716452.
130. Hoyt, F.; Alam, P.; Artikis, E.; Schwartz, C.L.; Hughson, A.G.; Race, B.; Baune, C.; Raymond, G.J.; Baron, G.S.; Kraus, A.; et al. Cryo-EM of prion strains from the same genotype of host identifies conformational determinants. *PLoS Pathog* **2022**, *18*, e1010947, doi:10.1371/journal.ppat.1010947.
131. Igel, A.; Fornara, B.; Rezaei, H.; Béringue, V. Prion assemblies: structural heterogeneity, mechanisms of formation, and role in species barrier. *Cell Tissue Res* **2023**, doi:10.1007/s00441-022-03700-2.
132. Sharma, A.; Bruce, K.L.; Chen, B.; Gyoneva, S.; Behrens, S.H.; Bommarius, A.S.; Chernoff, Y.O. Contributions of the Prion Protein Sequence, Strain, and Environment to the Species Barrier. *J Biol Chem* **2016**, *291*, 1277-1288, doi:10.1074/jbc.M115.684100.
133. Fändrich, M.; Meinhardt, J.; Grigorieff, N. Structural polymorphism of Alzheimer Abeta and other amyloid fibrils. *Prion* **2009**, *3*, 89-93.
134. Kodali, R.; Williams, A.D.; Chemuru, S.; Wetzel, R. Abeta(1-40) forms five distinct amyloid structures whose beta-sheet contents and fibril stabilities are correlated. *J Mol Biol* **2010**, *401*, 503-517, doi:10.1016/j.jmb.2010.06.023.
135. Fändrich, M.; Wulff, M.; Pedersen, J.S.; Otzen, D. Fibrillar Polymorphism In *Amyloid Fibrils and Prefibrillar Aggregates: Molecular and Biological Properties*, Otzen, D.E., Ed.; Wiley-VCH: Weinheim, 2013; pp. 321–343.
136. Tycko, R. Physical and structural basis for polymorphism in amyloid fibrils. *Protein Sci* **2014**, *23*, 1528-1539, doi:10.1002/pro.2544.
137. Lutter, L.; Serpell, C.J.; Tuite, M.F.; Xue, W.F. The molecular lifecycle of amyloid - Mechanism of assembly, mesoscopic organisation, polymorphism, suprastructures, and biological consequences. *Biochim Biophys Acta Proteins Proteom* **2019**, *1867*, 140257, doi:10.1016/j.bbapap.2019.07.010.
138. Arifin, M.I.; Hannaoui, S.; Chang, S.C.; Thapa, S.; Schatzl, H.M.; Gilch, S. Cervid Prion Protein Polymorphisms: Role in Chronic Wasting Disease Pathogenesis. *Int J Mol Sci* **2021**, *22*, 2271, doi:10.3390/ijms22052271.
139. Farzadfard, A.; Kunka, A.; Mason, T.O.; Larsen, J.A.; Norrild, R.K.; Dominguez, E.T.; Ray, S.; Buell, A.K. Thermodynamic characterization of amyloid polymorphism by microfluidic transient incomplete separation. *Chem Sci* **2024**, *15*, 2528-2544, doi:10.1039/d3sc05371g.
140. Pfeiffer, P.B.; Ugrina, M.; Schwierz, N.; Sigurdson, C.J.; Schmidt, M.; Fändrich, M. Cryo-EM Analysis of the Effect of Seeding with Brain-derived Abeta Amyloid Fibrils. *J Mol Biol* **2024**, *436*, 168422, doi:10.1016/j.jmb.2023.168422.
141. Mishra, S. Emerging Trends in Cryo-EM-based Structural Studies of Neuropathological Amyloids. *J Mol Biol* **2023**, *435*, 168361, doi:10.1016/j.jmb.2023.168361.
142. Petkova, A.T.; Leapman, R.D.; Guo, Z.; Yau, W.M.; Mattson, M.P.; Tycko, R. Self-propagating, molecular-level polymorphism in Alzheimer's beta-amyloid fibrils. *Science* **2005**, *307*, 262-265, doi:10.1126/science.1105850.
143. Peccati, F.; Pantaleone, S.; Solans-Monfort, X.; Sodupe, M. Fluorescent Markers for Amyloid-beta Detection: Computational Insights. *Isr J Chem* **2017**, *57*, 686-698, doi:10.1002/ijch.201600114.
144. Peccati, F.; Pantaleone, S.; Riffet, V.; Solans-Monfort, X.; Contreras-Garcia, J.; Guallar, V.; Sodupe, M. Binding of Thioflavin T and Related Probes to Polymorphic Models of Amyloid-beta Fibrils. *J Phys Chem B* **2017**, *121*, 8926-8934, doi:10.1021/acs.jpcb.7b06675.
145. Shorter, J.; Lindquist, S. Prions as adaptive conduits of memory and inheritance. *Nat Rev Genet* **2005**, *6*, 435-450, doi:10.1038/nrg1616.

146. Wiltzius, J.J.W.; Landau, M.; Nelson, R.; Sawaya, M.R.; Apostol, M.I.; Goldschmidt, L.; Soriaga, A.B.; Cascio, D.; Rajashankar, K.; Eisenberg, D. Molecular mechanisms for protein-encoded inheritance. *Nat Struct Mol Biol* **2009**, *16*, 973-978, doi:10.1038/nsmb.1643.
147. Liebman, S.W.; Chernoff, Y.O. Prions in yeast. *Genetics* **2012**, *191*, 1041-1072, doi:10.1534/genetics.111.137760.
148. Wickner, R.B.; Shewmaker, F.P.; Bateman, D.A.; Edskes, H.K.; Gorkovskiy, A.; Dayani, Y.; Bezsonov, E.E. Yeast prions: structure, biology, and prion-handling systems. *Microbiol Mol Biol Rev* **2015**, *79*, 1-17, doi:10.1128/MMBR.00041-14.
149. Wickner, R.B.; Edskes, H.K.; Gorkovskiy, A.; Bezsonov, E.E.; Stroobant, E.E. Yeast and Fungal Prions: Amyloid-Handling Systems, Amyloid Structure, and Prion Biology. *Adv Genet* **2016**, *93*, 191-236, doi:10.1016/bs.adgen.2015.12.003.
150. Bao, J.; Wen, Z.; Kim, M.; Zhao, X.; Lee, B.N.; Jung, S.H.; Davatzikos, C.; Saykin, A.J.; Thompson, P.M.; Kim, D.; et al. Identifying highly heritable brain amyloid phenotypes through mining Alzheimer's imaging and sequencing biobank data. *Pac Symp Biocomput* **2022**, *27*, 109-120.
151. Telling, G.C. The shape of things to come: structural insights into how prion proteins encipher heritable information. *Nat Commun* **2022**, *13*, 4003, doi:10.1038/s41467-022-31460-8.
152. Jarrett, J.T.; Lansbury, P.T., Jr. Seeding "one-dimensional crystallization" of amyloid: a pathogenic mechanism in Alzheimer's disease and scrapie? *Cell* **1993**, *73*, 1055-1058, doi:10.1016/0092-8674(93)90635-4.
153. Luers, L.; Bannach, O.; Stöhr, J.; Wördehoff, M.M.; Wolff, M.; Nagel-Steger, L.; Riesner, D.; Willbold, D.; Birkmann, E. Seeded fibrillation as molecular basis of the species barrier in human prion diseases. *PLoS One* **2013**, *8*, e72623, doi:10.1371/journal.pone.0072623.
154. Pinotsi, D.; Michel, C.H.; Buell, A.K.; Laine, R.F.; Mahou, P.; Dobson, C.M.; Kaminski, C.F.; Kaminski Schierle, G.S. Nanoscopic insights into seeding mechanisms and toxicity of alpha-synuclein species in neurons. *Proc Natl Acad Sci* **2016**, *113*, 3815-3819, doi:10.1073/pnas.1516546113.
155. Kaufman, S.K.; Thomas, T.L.; Del Tredici, K.; Braak, H.; Diamond, M.I. Characterization of tau prion seeding activity and strains from formaldehyde-fixed tissue. *Acta Neuropathol Commun* **2017**, *5*, 41, doi:10.1186/s40478-017-0442-8.
156. Mudher, A.; Colin, M.; Dujardin, S.; Medina, M.; Dewachter, I.; Alavi Naini, S.M.; Mandelkow, E.M.; Mandelkow, E.; Buée, L.; Goedert, M.; et al. What is the evidence that tau pathology spreads through prion-like propagation? *Acta Neuropathol Commun* **2017**, *5*, 99, doi:10.1186/s40478-017-0488-7.
157. Manca, M.; Kraus, A. Defining the Protein Seeds of Neurodegeneration using Real-Time Quaking-Induced Conversion Assays. *Biomolecules* **2020**, *10*, doi:10.3390/biom10091233.
158. Peng, C.; Trojanowski, J.Q.; Lee, V.M. Protein transmission in neurodegenerative disease. *Nat Rev Neurol* **2020**, *16*, 199-212, doi:10.1038/s41582-020-0333-7.
159. Standke, H.G.; Kraus, A. Seed amplification and RT-QuIC assays to investigate protein seed structures and strains. *Cell Tissue Res* **2022**, doi:10.1007/s00441-022-03595-z.
160. Thacker, D.; Sanagavarapu, K.; Frohm, B.; Meisl, G.; Knowles, T.P.J.; Linse, S. The role of fibril structure and surface hydrophobicity in secondary nucleation of amyloid fibrils. *Proc Natl Acad Sci U S A* **2020**, *117*, 25272-25283, doi:10.1073/pnas.2002956117.
161. Coysh, T.; Mead, S. The Future of Seed Amplification Assays and Clinical Trials. *Front Aging Neurosci* **2022**, *14*, 872629, doi:10.3389/fnagi.2022.872629.
162. Vaneyck, J.; Yousif, T.A.; Segers-Nolten, I.; Blum, C.; Claessens, M.M.A.E. Quantitative Seed Amplification Assay: A Proof-of-Principle Study. *J Phys Chem B* **2023**, *127*, 1735-1743, doi:10.1021/acs.jpcb.2c08326.
163. Sulskis, D.; Sneideriene, G.; Ziaunys, M.; Smirnovas, V. The seeding barrier between human and Syrian hamster prion protein amyloid fibrils is determined by beta2-alpha2 loop sequence elements. *Int J Biol Macromol* **2023**, *238*, 124038, doi:10.1016/j.ijbiomac.2023.124038.

164. Scheres, S.H.W.; Ryskeldi-Falcon, B.; Goedert, M. Molecular pathology of neurodegenerative diseases by cryo-EM of amyloids. *Nature* **2023**, *621*, 701-710, doi:10.1038/s41586-023-06437-2.
165. Yang, Y.; Arseni, D.; Zhang, W.; Huang, M.; Lovestam, S.; Schweighauser, M.; Kotecha, A.; Murzin, A.G.; Peak-Chew, S.Y.; Macdonald, J.; et al. Cryo-EM structures of amyloid-beta 42 filaments from human brains. *Science* **2022**, *375*, 167-172, doi:10.1126/science.abm7285.
166. Heerde, T.; Rennegarbe, M.; Biedermann, A.; Savran, D.; Pfeiffer, P.B.; Hitzenberger, M.; Baur, J.; Puscalau-Girtu, I.; Zacharias, M.; Schwierz, N.; et al. Cryo-EM demonstrates the in vitro proliferation of an ex vivo amyloid fibril morphology by seeding. *Nat Commun* **2022**, *13*, 85, doi:10.1038/s41467-021-27688-5.
167. Bondarev, S.A.; Antonets, K.S.; Kajava, A.V.; Nizhnikov, A.A.; Zhouravleva, G.A. Protein Co-Aggregation Related to Amyloids: Methods of Investigation, Diversity, and Classification. *Int J Mol Sci* **2018**, *19*, 2292, doi:10.3390/ijms19082292.
168. Sidhu, A.; Segers-Nolten, I.; Subramaniam, V. Conformational Compatibility Is Essential for Heterologous Aggregation of alpha-Synuclein. *ACS Chem Neurosci* **2016**, *7*, 719-727, doi:10.1021/acschemneuro.5b00322.
169. Ivanova, M.I.; Lin, Y.; Lee, Y.H.; Zheng, J.; Ramamoorthy, A. Biophysical processes underlying cross-seeding in amyloid aggregation and implications in amyloid pathology. *Biophys Chem* **2021**, *269*, 106507, doi:10.1016/j.bpc.2020.106507.
170. Subedi, S.; Sasidharan, S.; Nag, N.; Saudagar, P.; Tripathi, T. Amyloid Cross-Seeding: Mechanism, Implication, and Inhibition. *Molecules* **2022**, *27*, 1776, doi:10.3390/molecules27061776.
171. Chatterjee, D.; Jacob, R.S.; Ray, S.; Navalkar, A.; Singh, N.; Sengupta, S.; Gadhe, L.; Kadu, P.; Datta, D.; Paul, A.; et al. Co-aggregation and secondary nucleation in the life cycle of human prolactin/galanin functional amyloids. *Elife* **2022**, *11*, doi:10.7554/eLife.73835.
172. Semerdzhiev, S.A.; Segers-Nolten, I.; van der Schoot, P.; Blum, C.; Claessens, M.M.S.E. SARS-CoV-2 N-protein induces the formation of composite alpha-synuclein/N-protein fibrils that transform into a strain of alpha-synuclein fibrils. *Nanoscale* **2023**, *15*, 18337-18346, doi:10.1039/d3nr03556e.
173. Willbold, D.; Strodel, B.; Schroder, G.F.; Hoyer, W.; Heise, H. Amyloid-type Protein Aggregation and Prion-like Properties of Amyloids. *Chem Rev* **2021**, *121*, 8285-8307, doi:10.1021/acs.chemrev.1c00196.
174. Zielinski, M.; Röder, C.; Schröder, G.F. Challenges in sample preparation and structure determination of amyloids by cryo-EM. *J Biol Chem* **2021**, *297*, 100938, doi:10.1016/j.jbc.2021.100938.
175. Pretorius, E.; Vlok, M.; Venter, C.; Bezuidenhout, J.A.; Laubscher, G.J.; Steenkamp, J.; Kell, D.B. Persistent clotting protein pathology in Long COVID/ Post-Acute Sequelae of COVID-19 (PASC) is accompanied by increased levels of antiplasmin. *Cardiovasc Diabetol* **2021**, *20*, 172.
176. Turner, S.; Khan, M.A.; Putrino, D.; Woodcock, A.; Kell, D.B.; Pretorius, E. Long COVID: pathophysiological factors and abnormal coagulation. *Trends Endocrinol Metab* **2023**, *34*, 321-344, doi:https://doi.org/10.1016/j.tem.2023.03.002.
177. Turner, S.; Laubscher, G.J.; Khan, M.A.; Kell, D.B.; Pretorius, E. Accelerating discovery: A novel flow cytometric method for detecting fibrin(ogen) amyloid microclots using long COVID as a model *Heliyon* **2023**, *9*, e19605, doi:https://doi.org/10.1016/j.heliyon.2023.e19605.
178. Turner, S.; Naidoo, C.A.; Usher, T.J.; Kruger, A.; Venter, C.; Laubscher, G.J.; Khan, M.A.; Kell, D.B.; Pretorius, E. Increased Levels of Inflammatory and Endothelial Biomarkers in Blood of Long COVID Patients Point to Thrombotic Endothelialitis. *Semin Thromb Hemost* **2023**, doi:10.1055/s-0043-1769014.
179. Dalton, C.F.; de Oliveira, M.I.R.; Stafford, P.; Peake, N.; Kane, B.; Higham, A.; Singh, D.; Jackson, N.; Davies, H.; Price, D.; et al. Increased fibrinaloid microclot counts in platelet-poor plasma are associated with Long COVID. *medRxiv* **2024**, 2024.2004.2004.24305318, doi:10.1101/2024.04.04.24305318.

180. Nunes, J.M.; Kruger, A.; Proal, A.; Kell, D.B.; Pretorius, E. The Occurrence of Hyperactivated Platelets and Fibrinaloid Microclots in Myalgic Encephalomyelitis/Chronic Fatigue Syndrome (ME/CFS). *Pharmaceuticals (Basel)* **2022**, *15*, 931, doi:10.3390/ph15080931.
181. Nunes, J.M.; Kell, D.B.; Pretorius, E. Cardiovascular and haematological pathology in Myalgic Encephalomyelitis/Chronic Fatigue Syndrome (ME/CFS): a role for Viruses. *Blood Rev* **2023**, *60*, 101075, doi:10.1016/j.blre.2023.101075.
182. Grobbelaar, L.M.; Kruger, A.; Venter, C.; Burger, E.M.; Laubscher, G.J.; Maponga, T.G.; Kotze, M.J.; Kwaan, H.C.; Miller, J.B.; Fulkerson, D.; et al. Relative hypercoagulopathy of the SARS-CoV-2 Beta and Delta variants when compared to the less severe Omicron variants is related to TEG parameters, the extent of fibrin amyloid microclots, and the severity of clinical illness. *Semin Thromb Haemost* **2022**, *48*, 858-868, doi:10.1055/s-0042-1756306.
183. Pretorius, E.; Kell, D.B. A perspective on how microscopy imaging of fibrinaloid microclots and platelet pathology may be applied in clinical investigations. *Semin Thromb Haemost* **2023**, doi:10.1055/s-0043-1774796.
184. Kell, D.B.; Laubscher, G.J.; Pretorius, E. A central role for amyloid fibrin microclots in long COVID/PASC: origins and therapeutic implications. *Biochem J* **2022**, *479*, 537-559, doi:https://doi.org/10.1042/BCJ20220016.
185. Kell, D.B.; Pretorius, E. The potential role of ischaemia-reperfusion injury in chronic, relapsing diseases such as rheumatoid arthritis, long COVID and ME/CFS: evidence, mechanisms, and therapeutic implications. *Biochem J* **2022**, *479*, 1653-1708.
186. Kell, D.B.; Khan, M.A.; Kane, B.; Lip, G.Y.H.; Pretorius, E. The role of fibrinaloid microclots in Postural Orthostatic Tachycardia Syndrome (POTS): focus on Long COVID. *J Personalised Medicine* **2024**, *14*, 170, doi:https://doi.org/10.3390/jpm14020170.
187. Schofield, J.; Abrams, S.T.; Jenkins, R.; Lane, S.; Wang, G.; Toh, C.H. Amyloid-fibrinogen aggregates ("microclots") predict risks of Disseminated Intravascular Coagulation and mortality. *Blood Adv* **2024**, doi:10.1182/bloodadvances.2023012473.
188. Appelman, B.; Charlton, B.T.; Goulding, R.P.; Kerkhoff, T.J.; Breedveld, E.A.; Noort, W.; Offringa, C.; Bloemers, F.W.; van Weeghel, M.; Schomakers, B.V.; et al. Muscle abnormalities worsen after post-exertional malaise in long COVID. *Nat Commun* **2024**, *15*, 17, doi:10.1038/s41467-023-44432-3.
189. Thagard, P. Explaining disease: Correlations, causes, and mechanisms. *Minds and Machines* **1998**, *8*, 61-78.
190. Thagard, P. *How scientists explain disease*; Princeton University Press: Princeton, NJ, 1999.
191. Thagard, P. Coherence, truth, and the development of scientific knowledge. *Philosophy of Science* **2007**, *74*, 28-47.
192. Thagard, P. Explanatory Coherence. *Reasoning: Studies of Human Inference and Its Foundations* **2008**, 471-513.
193. Nelson, R.; Sawaya, M.R.; Balbirnie, M.; Madsen, A.O.; Riekel, C.; Grothe, R.; Eisenberg, D. Structure of the cross-beta spine of amyloid-like fibrils. *Nature* **2005**, *435*, 773-778, doi:10.1038/nature03680.
194. Tycko, R.; Wickner, R.B. Molecular structures of amyloid and prion fibrils: consensus versus controversy. *Acc Chem Res* **2013**, *46*, 1487-1496, doi:10.1021/ar300282r.
195. Serpell, L.C.; Sunde, M.; Benson, M.D.; Tennent, G.A.; Pepys, M.B.; Fraser, P.E. The protofilament substructure of amyloid fibrils. *J Mol Biol* **2000**, *300*, 1033-1039, doi:10.1006/jmbi.2000.3908.
196. Jahn, T.R.; Makin, O.S.; Morris, K.L.; Marshall, K.E.; Tian, P.; Sikorski, P.; Serpell, L.C. The common architecture of cross-beta amyloid. *J Mol Biol* **2010**, *395*, 717-727, doi:10.1016/j.jmb.2009.09.039.
197. Morris, K.L.; Serpell, L.C. From Molecular to Supramolecular Amyloid Structures: Contributions from Fiber Diffraction and Electron Microscopy. In *Amyloid Fibrils and Prefibrillar Aggregates: Molecular and Biological Properties*, Otzen, D.E., Ed.; Wiley-VCH: Weinheim, 2013; pp. 63-84.
198. Iadanza, M.G.; Jackson, M.P.; Hewitt, E.W.; Ranson, N.A.; Radford, S.E. A new era for understanding amyloid structures and disease. *Nat Rev Mol Cell Bio* **2018**, *19*, 755-773, doi:10.1038/s41580-018-0060-8.

199. Thurber, K.R.; Yau, W.M.; Tycko, R. Structure of Amyloid Peptide Ribbons Characterized by Electron Microscopy, Atomic Force Microscopy, and Solid-State Nuclear Magnetic Resonance. *J Phys Chem B* **2024**, *128*, 1711-1723, doi:10.1021/acs.jpcb.3c07867.
200. Gremer, L.; Scholzel, D.; Schenk, C.; Reinartz, E.; Labahn, J.; Ravelli, R.B.G.; Tusche, M.; Lopez-Iglesias, C.; Hoyer, W.; Heise, H.; et al. Fibril structure of amyloid-beta(1-42) by cryo-electron microscopy. *Science* **2017**, *358*, 116-119, doi:10.1126/science.aao2825.
201. Chen, G.F.; Xu, T.H.; Yan, Y.; Zhou, Y.R.; Jiang, Y.; Melcher, K.; Xu, H.E. Amyloid beta: structure, biology and structure-based therapeutic development. *Acta Pharmacol Sin* **2017**, *38*, 1205-1235, doi:10.1038/aps.2017.28.
202. Gallardo, R.; Ranson, N.A.; Radford, S.E. Amyloid structures: much more than just a cross-beta fold. *Curr Opin Struct Biol* **2020**, *60*, 7-16, doi:10.1016/j.sbi.2019.09.001.
203. Greenwald, J.; Riek, R. Biology of amyloid: structure, function, and regulation. *Structure* **2010**, *18*, 1244-1260, doi:10.1016/j.str.2010.08.009.
204. Fändrich, M.; Schmidt, M.; Grigorieff, N. Recent progress in understanding Alzheimer's beta-amyloid structures. *Trends Biochem Sci* **2011**, *36*, 338-345, doi:10.1016/j.tibs.2011.02.002.
205. Eisenberg, D.S.; Sawaya, M.R. Structural Studies of Amyloid Proteins at the Molecular Level. *Annu Rev Biochem* **2017**, *86*, 69-95, doi:10.1146/annurev-biochem-061516-045104.
206. Heerde, T.; Bansal, A.; Schmidt, M.; Fändrich, M. Cryo-EM structure of a catalytic amyloid fibril. *Sci Rep* **2023**, *13*, 4070, doi:10.1038/s41598-023-30711-y.
207. Heerde, T.; Schütz, D.; Lin, Y.J.; Münch, J.; Schmidt, M.; Fändrich, M. Cryo-EM structure and polymorphic maturation of a viral transduction enhancing amyloid fibril. *Nat Commun* **2023**, *14*, 4293, doi:10.1038/s41467-023-40042-1.
208. Gonay, V.; Dunne, M.P.; Caceres-Delpiano, J.; Kajava, A.V. Developing machine-learning-based amyloid predictors with Cross-Beta DB. *bioRxiv* **2024**, 2024.2002.2012.579644, doi:10.1101/2024.02.12.579644.
209. Bücker, R.; Seuring, C.; Cazey, C.; Veith, K.; Garcia-Alai, M.; Grünewald, K.; Landau, M. The Cryo-EM structures of two amphibian antimicrobial cross-beta amyloid fibrils. *Nat Commun* **2022**, *13*, 4356, doi:10.1038/s41467-022-32039-z.
210. Khurana, R.; Coleman, C.; Ionescu-Zanetti, C.; Carter, S.A.; Krishna, V.; Grover, R.K.; Roy, R.; Singh, S. Mechanism of thioflavin T binding to amyloid fibrils. *J Struct Biol* **2005**, *151*, 229-238, doi:10.1016/j.jsb.2005.06.006.
211. Hawe, A.; Sutter, M.; Jiskoot, W. Extrinsic fluorescent dyes as tools for protein characterization. *Pharm Res* **2008**, *25*, 1487-1499, doi:10.1007/s11095-007-9516-9.
212. Amdursky, N.; Erez, Y.; Huppert, D. Molecular rotors: what lies behind the high sensitivity of the thioflavin-T fluorescent marker. *Acc Chem Res* **2012**, *45*, 1548-1557, doi:10.1021/ar300053p.
213. Biancalana, M.; Koide, S. Molecular mechanism of Thioflavin-T binding to amyloid fibrils. *Biochim Biophys Acta* **2010**, *1804*, 1405-1412, doi:10.1016/j.bbapap.2010.04.001.
214. Gade Malmos, K.; Blancas-Mejia, L.M.; Weber, B.; Buchner, J.; Ramirez-Alvarado, M.; Naiki, H.; Otzen, D. ThT 101: a primer on the use of thioflavin T to investigate amyloid formation. *Amyloid* **2017**, *24*, 1-16, doi:10.1080/13506129.2017.1304905.
215. Lee, J.E.; Sang, J.C.; Rodrigues, M.; Carr, A.R.; Horrocks, M.H.; De, S.; Bongiovanni, M.N.; Flagmeier, P.; Dobson, C.M.; Wales, D.J.; et al. Mapping Surface Hydrophobicity of alpha-Synuclein Oligomers at the Nanoscale. *Nano Lett* **2018**, *18*, 7494-7501, doi:10.1021/acs.nanolett.8b02916.
216. Taylor, C.G.; Meisl, G.; Horrocks, M.H.; Zetterberg, H.; Knowles, T.P.J.; Klenerman, D. Extrinsic Amyloid-Binding Dyes for Detection of Individual Protein Aggregates in Solution. *Anal Chem* **2018**, *90*, 10385-10393, doi:10.1021/acs.analchem.8b02226.

743 217. De, S.; Klenerman, D. Imaging individual protein aggregates to follow aggregation and determine the role of aggregates in
744 neurodegenerative disease. *Biochim Biophys Acta Proteins Proteom* **2019**, *1867*, 870-878, doi:10.1016/j.bbapap.2018.12.010.
745 218. Sulatskaya, A.I.; Rychkov, G.N.; Sulatsky, M.I.; Mikhailova, E.V.; Melnikova, N.M.; Andozhskaya, V.S.; Kuznetsova, I.M.;
746 Turoverov, K.K. New Evidence on a Distinction between A beta 40 and A beta 42 Amyloids: Thioflavin T Binding Modes,
747 Clustering Tendency, Degradation Resistance, and Cross-Seeding. *Int J Mol Sci* **2022**, *23*, 5513.
748 219. Xue, C.; Lin, T.Y.; Chang, D.; Guo, Z. Thioflavin T as an amyloid dye: fibril quantification, optimal concentration and
749 effect on aggregation. *R Soc Open Sci* **2017**, *4*, 160696, doi:10.1098/rsos.160696.
750 220. Arad, E.; Green, H.; Jelinek, R.; Rapaport, H. Revisiting thioflavin T (ThT) fluorescence as a marker of protein fibrillation -
751 The prominent role of electrostatic interactions. *J Colloid Interface Sci* **2020**, *573*, 87-95, doi:10.1016/j.jcis.2020.03.075.
752 221. Lucignano, R.; Spadaccini, R.; Merlino, A.; Ami, D.; Natalello, A.; Ferraro, G.; Picone, D. Structural insights and
753 aggregation propensity of a super-stable monellin mutant: A new potential building block for protein-based
754 nanostructured materials. *Int J Biol Macromol* **2024**, *254*, 127775, doi:10.1016/j.ijbiomac.2023.127775.
755 222. Pujols, J.; Peña-Díaz, S.; Lázaro, D.F.; Peccati, F.; Pinheiro, F.; González, D.; Carija, A.; Navarro, S.; Conde-Giménez, M.;
756 García, J.; et al. Small molecule inhibits alpha-synuclein aggregation, disrupts amyloid fibrils, and prevents degeneration
757 of dopaminergic neurons. *Proc Natl Acad Sci U S A* **2018**, *115*, 10481-10486, doi:10.1073/pnas.1804198115.
758 223. Bertoncini, C.W.; Celej, M.S. Small molecule fluorescent probes for the detection of amyloid self-assembly *in vitro* and *in*
759 *vivo*. *Curr Protein Pept Sci* **2011**, *12*, 205-220.
760 224. Panda, C.; Sharma, L.G.; Pandey, L.M. Experimental procedures to investigate fibrillation of proteins. *MethodsX* **2023**, *11*,
761 102445, doi:10.1016/j.mex.2023.102445.
762 225. Choo, L.P.; Wetzel, D.L.; Halliday, W.C.; Jackson, M.; LeVine, S.M.; Mantsch, H.H. *In situ* characterization of beta-amyloid
763 in Alzheimer's diseased tissue by synchrotron Fourier transform infrared microspectroscopy. *Biophys J* **1996**, *71*, 1672-1679,
764 doi:10.1016/S0006-3495(96)79411-0.
765 226. Cerdà-Costa, N.; De la Arada, I.; Avilés, F.X.; Arrondo, J.L.; Villegas, S. Influence of aggregation propensity and stability
766 on amyloid fibril formation as studied by Fourier transform infrared spectroscopy and two-dimensional COS analysis.
767 *Biochemistry* **2009**, *48*, 10582-10590, doi:10.1021/bi900960s.
768 227. Prater, C.; Bai, Y.; Konings, S.C.; Martinsson, I.; Swaminathan, V.S.; Nordenfelt, P.; Gouras, G.; Borondics, F.; Klementieva,
769 O. Fluorescently Guided Optical Photothermal Infrared Microspectroscopy for Protein-Specific Bioimaging at Subcellular
770 Level. *J Med Chem* **2023**, *66*, 2542-2549, doi:10.1021/acs.jmedchem.2c01359.
771 228. Zhang, G.; Babenko, V.; Dzwolak, W.; Keiderling, T.A. Dimethyl Sulfoxide Induced Destabilization and Disassembly of
772 Various Structural Variants of Insulin Fibrils Monitored by Vibrational Circular Dichroism. *Biochemistry* **2015**, *54*,
773 7193-7202, doi:10.1021/acs.biochem.5b00809.
774 229. Cornejo, A.; Aguilar Sandoval, F.; Caballero, L.; Machuca, L.; Munoz, P.; Caballero, J.; Perry, G.; Ardiles, A.; Areche, C.;
775 Melo, F. Rosmarinic acid prevents fibrillization and diminishes vibrational modes associated to beta sheet in tau protein
776 linked to Alzheimer's disease. *J Enzyme Inhib Med Chem* **2017**, *32*, 945-953, doi:10.1080/14756366.2017.1347783.
777 230. Li, S.; Luo, Z.; Zhang, R.; Xu, H.; Zhou, T.; Liu, L.; Qu, J. Distinguishing Amyloid beta-Protein in a Mouse Model of
778 Alzheimer's Disease by Label-Free Vibrational Imaging. *Biosensors (Basel)* **2021**, *11*, 365, doi:10.3390/bios11100365.
779 231. Watson, M.D.; Lee, J.C. Coupling chemical biology and vibrational spectroscopy for studies of amyloids in vitro and in
780 cells. *Curr Opin Chem Biol* **2021**, *64*, 90-97, doi:10.1016/j.cbpa.2021.05.005.
781 232. Ami, D.; Natalello, A. Characterization of the Conformational Properties of Soluble and Insoluble Proteins by Fourier
782 Transform Infrared Spectroscopy. *Methods Mol Biol* **2022**, *2406*, 439-454, doi:10.1007/978-1-0716-1859-2_26.

233. Vu, K.H.P.; Blankenburg, G.H.; Lesser-Rojas, L.; Chou, C.F. Applications of Single-Molecule Vibrational Spectroscopic Techniques for the Structural Investigation of Amyloid Oligomers. *Molecules* **2022**, *27*, 6448, doi:10.3390/molecules27196448.

234. Ami, D.; Mereghetti, P.; Natalello, A. Contribution of Infrared Spectroscopy to the Understanding of Amyloid Protein Aggregation in Complex Systems. *Front Mol Biosci* **2022**, *9*, 822852, doi:10.3389/fmolb.2022.822852.

235. de la Arada, I.; Seiler, C.; Mantele, W. Amyloid fibril formation from human and bovine serum albumin followed by quasi-simultaneous Fourier-transform infrared (FT-IR) spectroscopy and static light scattering (SLS). *Eur Biophys J* **2012**, *41*, 931-938, doi:10.1007/s00249-012-0845-1.

236. Ridgley, D.M.; Claunch, E.C.; Barone, J.R. Characterization of large amyloid fibers and tapes with Fourier transform infrared (FT-IR) and Raman spectroscopy. *Appl Spectrosc* **2013**, *67*, 1417-1426, doi:10.1366/13-07059.

237. Biancalana, M.; Makabe, K.; Koide, A.; Koide, S. Molecular mechanism of thioflavin-T binding to the surface of beta-rich peptide self-assemblies. *J Mol Biol* **2009**, *385*, 1052-1063, doi:10.1016/j.jmb.2008.11.006.

238. Sidhu, A.; Vaneyck, J.; Blum, C.; Segers-Nolten, I.; Subramaniam, V. Polymorph-specific distribution of binding sites determines thioflavin-T fluorescence intensity in alpha-synuclein fibrils. *Amyloid* **2018**, *25*, 189-196, doi:10.1080/13506129.2018.1517736.

239. Chisholm, T.S.; Hunter, C.A. A closer look at amyloid ligands, and what they tell us about protein aggregates. *Chem Soc Rev* **2024**, *53*, 1354-1374, doi:10.1039/d3cs00518f.

240. Rovnyagina, N.R.; Sluchanko, N.N.; Tikhonova, T.N.; Fadeev, V.V.; Litskevich, A.Y.; Maskevich, A.A.; Shirshin, E.A. Binding of thioflavin T by albumins: An underestimated role of protein oligomeric heterogeneity. *Int J Biol Macromol* **2018**, *108*, 284-290, doi:10.1016/j.ijbiomac.2017.12.002.

241. Rovnyagina, N.R.; Budylin, G.S.; Vainer, Y.G.; Tikhonova, T.N.; Vasin, S.L.; Yakovlev, A.A.; Kompanets, V.O.; Chekalin, S.V.; Priezzhev, A.V.; Shirshin, E.A. Fluorescence Lifetime and Intensity of Thioflavin T as Reporters of Different Fibrillation Stages: Insights Obtained from Fluorescence Up-Conversion and Particle Size Distribution Measurements. *Int J Mol Sci* **2020**, *21*, 6169, doi:10.3390/ijms21176169.

242. Rovnyagina, N.R.; Tikhonova, T.N.; Kompanets, V.O.; Sluchanko, N.N.; Tugaeva, K.V.; Chekalin, S.V.; Fadeev, V.V.; Lademann, J.; Darvin, M.E.; Shirshi, E.A. Free and bound Thioflavin T molecules with ultrafast relaxation: implications for assessment of protein binding and aggregation. *Laser Phys Lett* **2019**, *16*, 075601, doi:https://doi.org/10.1088/1612-202X/ab2244.

243. Mikalauskaite, K.; Ziaunys, M.; Sneideris, T.; Smirnovas, V. Effect of Ionic Strength on Thioflavin-T Affinity to Amyloid Fibrils and Its Fluorescence Intensity. *Int J Mol Sci* **2020**, *21*, 8916, doi:10.3390/ijms21238916.

244. Ziaunys, M.; Sakalauskas, A.; Mikalauskaite, K.; Smirnovas, V. Exploring the occurrence of thioflavin-T-positive insulin amyloid aggregation intermediates. *PeerJ* **2021**, *9*, e10918, doi:10.7717/peerj.10918.

245. Wolfe, L.S.; Calabrese, M.F.; Nath, A.; Blaho, D.V.; Miranker, A.D.; Xiong, Y. Protein-induced photophysical changes to the amyloid indicator dye thioflavin T. *Proc Natl Acad Sci* **2010**, *107*, 16863-16868, doi:10.1073/pnas.1002867107.

246. Ziaunys, M.; Smirnovas, V. Additional Thioflavin-T Binding Mode in Insulin Fibril Inner Core Region. *J Phys Chem B* **2019**, *123*, 8727-8732, doi:10.1021/acs.jpcb.9b08652.

247. Ziaunys, M.; Mikalauskaite, K.; Sakalauskas, A.; Smirnovas, V. Investigating lysozyme amyloid fibril formation and structural variability dependence on its initial folding state under different pH conditions. *Protein Sci* **2024**, *33*, e4888, doi:10.1002/pro.4888.

248. Chaari, A.; Fahy, C.; Chevillot-Biraud, A.; Rholam, M. Investigating the effects of different natural molecules on the structure and oligomerization propensity of hen egg-white lysozyme. *Int J Biol Macromol* **2019**, *134*, 189-201, doi:10.1016/j.ijbiomac.2019.05.048.

249. Anselmo, S.; Sancataldo, G.; Vetri, V. Deciphering amyloid fibril molecular maturation through FLIM-phasor analysis of thioflavin T. *Biophys Rep (N Y)* **2024**, *4*, 100145, doi:10.1016/j.bpr.2024.100145.
250. Lindberg, D.J.; Wranne, M.S.; Gilbert Gatty, M.; Westerlund, F.; Esbjörner, E.K. Steady-state and time-resolved Thioflavin-T fluorescence can report on morphological differences in amyloid fibrils formed by Abeta(1-40) and Abeta(1-42). *Biochem Biophys Res Commun* **2015**, *458*, 418-423, doi:10.1016/j.bbrc.2015.01.132.
251. Sulatskaya, A.I.; Rodina, N.P.; Polyakov, D.S.; Sulatsky, M.I.; Artamonova, T.O.; Khodorkovskii, M.A.; Shavlovsky, M.M.; Kuznetsova, I.M.; Turoverov, K.K. Structural Features of Amyloid Fibrils Formed from the Full-Length and Truncated Forms of Beta-2-Microglobulin Probed by Fluorescent Dye Thioflavin T. *Int J Mol Sci* **2018**, *19*, 2762, doi:10.3390/ijms19092762.
252. De Luca, G.; Fennema Galparsoro, D.; Sancataldo, G.; Leone, M.; Fodera, V.; Vetri, V. Probing ensemble polymorphism and single aggregate structural heterogeneity in insulin amyloid self-assembly. *J Colloid Interface Sci* **2020**, *574*, 229-240, doi:10.1016/j.jcis.2020.03.107.
253. Thompson, A.J.; Herling, T.W.; Kubankova, M.; Vysniauskas, A.; Knowles, T.P.; Kuimova, M.K. Molecular Rotors Provide Insights into Microscopic Structural Changes During Protein Aggregation. *J Phys Chem B* **2015**, *119*, 10170-10179, doi:10.1021/acs.jpcb.5b05099.
254. Krebs, M.R.H.; Bromley, E.H.; Donald, A.M. The binding of thioflavin-T to amyloid fibrils: localisation and implications. *J Struct Biol* **2005**, *149*, 30-37, doi:10.1016/j.jsb.2004.08.002.
255. Noormägi, A.; Primar, K.; Tõugu, V.; Palumaa, P. Interference of low-molecular substances with the thioflavin-T fluorescence assay of amyloid fibrils. *J Pept Sci* **2012**, *18*, 59-64, doi:10.1002/psc.1416.
256. Hulscher, N.; Procter, B.C.; Wynn, C.; McCullough, P.A. Clinical Approach to Post-acute Sequelae After COVID-19 Infection and Vaccination. *Cureus* **2023**, *15*, e49204, doi:10.7759/cureus.49204.
257. McCullough, P.A.; Wynn, C.; Procter, B.C. Clinical Rationale for SARS-CoV-2 Base Spike Protein Detoxification in Post COVID-19 and Vaccine Injury Syndromes *J Amer Phys Surg* **2023**, *28*, 90-93.
258. Yang, M.; Wu, J.; Huang, Q.; Jia, Y. Probing the Role of Catalytic Triad on the Cleavage between Intramolecular Chaperone and NK Mature Peptide. *J Agric Food Chem* **2021**, *69*, 2348-2353, doi:10.1021/acs.jafc.0c07238.
259. Pan, X.; Liang, P.; Teng, L.; Ren, Y.; Peng, J.; Liu, W.; Yang, Y. Study on molecular mechanisms of nattokinase in pharmacological action based on label-free liquid chromatography-tandem mass spectrometry. *Food Sci Nutr* **2019**, *7*, 3185-3193, doi:10.1002/fsn3.1157.
260. Fujita, M.; Ito, Y.; Hong, K.; Nishimuro, S. Characterization of Nattokinase-degraded Products from Human Fibrinogen or Cross-linked Fibrin. *Fibrinolysis* **1995**, *9*, 157-164.
261. Tanikawa, T.; Kiba, Y.; Yu, J.; Hsu, K.; Chen, S.; Ishii, A.; Yokogawa, T.; Suzuki, R.; Inoue, Y.; Kitamura, M. Degradative Effect of Nattokinase on Spike Protein of SARS-CoV-2. *Molecules* **2022**, *27*, 5405.
262. Hsu, R.L.; Lee, K.T.; Wang, J.H.; Lee, L.Y.; Chen, R.P. Amyloid-degrading ability of nattokinase from *Bacillus subtilis* natto. *J Agric Food Chem* **2009**, *57*, 503-508, doi:10.1021/jf803072r.
263. Ni, A.; Li, H.; Wang, R.; Sun, R.; Zhang, Y. Degradation of amyloid β-peptides catalyzed by nattokinase *in vivo* and *in vitro*. *Food Sci Hum Wellness* **2023**, *12*, 1905-1916, doi: http://doi.org/10.1016/j.fshw.2023.02.042.
264. Naik, S.; Katariya, R.; Shelke, S.; Patravale, V.; Umekar, M.; Kotagale, N.; Taksande, B. Nattokinase prevents beta-amyloid peptide (Abeta(1-42)) induced neuropsychiatric complications, neuroinflammation and BDNF signalling disruption in mice. *Eur J Pharmacol* **2023**, *952*, 175821, doi:10.1016/j.ejphar.2023.175821.
265. Meisl, G.; Knowles, T.P.; Klenerman, D. The molecular processes underpinning prion-like spreading and seed amplification in protein aggregation. *Curr Opin Neurobiol* **2020**, *61*, 58-64, doi:10.1016/j.conb.2020.01.010.

266. Young, K.A.; Mancera, R.L. Review: Investigating the aggregation of amyloid beta with surface plasmon resonance: Do different approaches yield different results? *Anal Biochem* **2022**, *654*, 114828, doi:10.1016/j.ab.2022.114828.
267. Jan, A.; Gokce, O.; Luthi-Carter, R.; Lashuel, H.A. The ratio of monomeric to aggregated forms of Abeta40 and Abeta42 is an important determinant of amyloid-beta aggregation, fibrillogenesis, and toxicity. *J Biol Chem* **2008**, *283*, 28176-28189, doi:10.1074/jbc.M803159200.
268. Wang, L.; Eom, K.; Kwon, T. Different Aggregation Pathways and Structures for Abeta40 and Abeta42 Peptides. *Biomolecules* **2021**, *11*, 198, doi:10.3390/biom11020198.
269. Wei, G.; Su, Z.; Reynolds, N.P.; Arosio, P.; Hamley, I.W.; Gazit, E.; Mezzenga, R. Self-assembling peptide and protein amyloids: from structure to tailored function in nanotechnology. *Chem Soc Rev* **2017**, *46*, 4661-4708, doi:10.1039/c6cs00542j.
270. Tipping, K.W.; van Oosten-Hawle, P.; Hewitt, E.W.; Radford, S.E. Amyloid Fibres: Inert End-Stage Aggregates or Key Players in Disease? *Trends Biochem Sci* **2015**, *40*, 719-727, doi:10.1016/j.tibs.2015.10.002.
271. Tycko, R. Structure of aggregates revealed. *Nature* **2016**, *537*, 492-493, doi:10.1038/nature19470.
272. Bunce, S.J.; Wang, Y.; Stewart, K.L.; Ashcroft, A.E.; Radford, S.E.; Hall, C.K.; Wilson, A.J. Molecular insights into the surface-catalyzed secondary nucleation of amyloid-beta(40) (Abeta(40)) by the peptide fragment Abeta(16-22). *Sci Adv* **2019**, *5*, eaav8216, doi:10.1126/sciadv.aav8216.
273. Michaels, T.C.T.; Saric, A.; Habchi, J.; Chia, S.; Meisl, G.; Vendruscolo, M.; Dobson, C.M.; Knowles, T.P.J. Chemical Kinetics for Bridging Molecular Mechanisms and Macroscopic Measurements of Amyloid Fibril Formation. *Annu Rev Phys Chem* **2018**, *69*, 273-298, doi:10.1146/annurev-physchem-050317-021322.
274. Vaquer-Alicea, J.; Diamond, M.I. Propagation of Protein Aggregation in Neurodegenerative Diseases. *Annu Rev Biochem* **2019**, *88*, 785-810, doi:10.1146/annurev-biochem-061516-045049.
275. Ke, P.C.; Zhou, R.; Serpell, L.C.; Riek, R.; Knowles, T.P.J.; Lashuel, H.A.; Gazit, E.; Hamley, I.W.; Davis, T.P.; Fandrich, M.; et al. Half a century of amyloids: past, present and future. *Chem Soc Rev* **2020**, *49*, 5473-5509, doi:10.1039/c9cs00199a.
276. Hammarström, P.; Simon, R.; Nystrom, S.; Konradsson, P.; Åslund, A.; Nilsson, K.P.R. A fluorescent pentameric thiophene derivative detects in vitro-formed prefibrillar protein aggregates. *Biochemistry* **2010**, *49*, 6838-6845, doi:10.1021/bi100922r.
277. Klingstedt, T.; Nilsson, K.P.R. Luminescent conjugated poly- and oligo-thiophenes: optical ligands for spectral assignment of a plethora of protein aggregates. *Biochem Soc Trans* **2012**, *40*, 704-710, doi:10.1042/BST20120009.
278. König, C.; Skånberg, R.; Hotz, I.; Ynnerman, A.; Norman, P.; Linares, M. Binding sites for luminescent amyloid biomarkers from non-biased molecular dynamics simulations. *Chem Commun* **2018**, *54*, 3030-3033, doi:10.1039/c8cc00105g.
279. Nilsson, K.P.; Lindgren, M.; Hammarström, P. A pentameric luminescent-conjugated oligothiophene for optical imaging of in vitro-formed amyloid fibrils and protein aggregates in tissue sections. *Methods Mol Biol* **2012**, *849*, 425-434, doi:10.1007/978-1-61779-551-0_29.
280. Nyström, S.; Bäck, M.; Nilsson, K.P.R.; Hammarström, P. Imaging Amyloid Tissues Stained with Luminescent Conjugated Oligothiophenes by Hyperspectral Confocal Microscopy and Fluorescence Lifetime Imaging. *J Vis Exp* **2017**, 56279, doi:10.3791/56279.
281. Sjölander, D.; Bijzet, J.; Hazenberg, B.P.C.; Nilsson, K.P.; Hammarström, P. Sensitive and rapid assessment of amyloid by oligothiophene fluorescence in subcutaneous fat tissue. *Amyloid* **2015**, *22*, 19-25, doi:10.3109/13506129.2014.984063.
282. Petrlova, J.; Samsudin, F.; Bond, P.J.; Schmidtchen, A. SARS-CoV-2 spike protein aggregation is triggered by bacterial lipopolysaccharide. *FEBS Lett* **2022**, *596*, 2566-2575, doi:10.1002/1873-3468.14490.
283. Morten, M.J.; Sirvio, L.; Rupawala, H.; Mee Hayes, E.; Franco, A.; Radulescu, C.; Ying, L.; Barnes, S.J.; Muga, A.; Ye, Y. Quantitative super-resolution imaging of pathological aggregates reveals distinct toxicity profiles in different synucleinopathies. *Proc Natl Acad Sci U S A* **2022**, *119*, e2205591119, doi:10.1073/pnas.2205591119.

284. Currin, A.; Swainston, N.; Day, P.J.; Kell, D.B. Synthetic biology for the directed evolution of protein biocatalysts: navigating sequence space intelligently. *Chem Soc Rev* **2015**, *44*, 1172-1239, doi:10.1039/c1034cs00351a.
285. Metkar, S.K.; Girigoswami, A.; Murugesan, R.; Girigoswami, K. Lumbrokinase for degradation and reduction of amyloid fibrils associated with amyloidosis. *Journal of Applied Biomedicine* **2017**, *15*, 96-104.
286. Metkar, S.K.; Ghosh, S.; Girigoswami, A.; Girigoswami, K. The Potential of Serratiopetidase and Lumbrokinase for the Degradation of Prion Peptide 106-126 - an In Vitro and In Silico Perspective. *CNS Neurol Disord Drug Targets* **2019**, *18*, 723-731, doi:10.2174/1871527318666191021150002.
287. Metkar, S.K.; Girigoswami, A.; Vijayashree, R.; Girigoswami, K. Attenuation of subcutaneous insulin induced amyloid mass in vivo using Lumbrokinase and Serratiopeptidase. *Int J Biol Macromol* **2020**, *163*, 128-134, doi:10.1016/j.ijbiomac.2020.06.256.
288. Fadl, N.N.; Ahmed, H.H.; Booles, H.F.; Sayed, A.H. Serrapeptase and nattokinase intervention for relieving Alzheimer's disease pathophysiology in rat model. *Hum Exp Toxicol* **2013**, *32*, 721-735, doi:10.1177/0960327112467040.
289. Jadhav, S.B.; Shah, N.; Rathi, A.; Rathi, V.; Rathi, A. Serratiopeptidase: Insights into the therapeutic applications. *Biotechnol Rep (Amst)* **2020**, *28*, e00544, doi:10.1016/j.btre.2020.e00544.
290. Metkar, S.K.; Girigoswami, A.; Bondage, D.D.; Shinde, U.G.; Girigoswami, K. The potential of lumbrokinase and serratiopeptidase for the degradation of Aβ 1–42 peptide – an in vitro and in silico approach. *Int J Neurosci* **2024**, *134*, 112-123, doi:https://doi.org/10.1080/00207454.2022.2089137.
291. Liao, J.; Ren, X.; Yang, B.; Li, H.; Zhang, Y.; Yin, Z. Targeted thrombolysis by using c-RGD-modified N,N,N-Trimethyl Chitosan nanoparticles loaded with lumbrokinase. *Drug Dev Ind Pharm* **2019**, *45*, 88-95, doi:10.1080/03639045.2018.1522324.
292. Metkar, S.K.; Girigoswami, A.; Murugesan, R.; Girigoswami, K. *In vitro* and *in vivo* insulin amyloid degradation mediated by Serratiopeptidase. *Mater Sci Eng C Mater Biol Appl* **2017**, *70*, 728-735, doi:10.1016/j.msec.2016.09.049.
293. Nair, S.R.; C, S.D. Serratiopeptidase: An integrated View of Multifaceted Therapeutic Enzyme. *Biomolecules* **2022**, *12*, 1468, doi:10.3390/biom12101468.
294. Katsipis, G.; Avgoulas, D.I.; Geromichalos, G.D.; Petala, M.; Pantazaki, A.A. In vitro and in silico evaluation of the serrapeptase effect on biofilm and amyloids of *Pseudomonas aeruginosa*. *Appl Microbiol Biotechnol* **2023**, *107*, 7269-7285, doi:10.1007/s00253-023-12772-1.
295. Mei, J.f.; Cai, S.f.; Yi, Y.; Wang, X.D.; Ying, G.Q. Study of the fibrinolytic activity of serrapeptase and its *in vitro* thrombolytic effects. *Braz J Pharm Sci* **2022**, *58*, e201004, doi:https://doi.org/10.1590/s2175-97902022e201004.
296. Banerjee, G.; Ray, A.K. Impact of microbial proteases on biotechnological industries. *Biotechnol Genet Eng Rev* **2017**, *33*, 119-143, doi:10.1080/02648725.2017.1408256.
297. Ladner-Keay, C.L.; Griffith, B.J.; Wishart, D.S. Shaking alone induces *de novo* conversion of recombinant prion proteins to beta-sheet rich oligomers and fibrils. *PLoS One* **2014**, *9*, e98753, doi:10.1371/journal.pone.0098753.
298. Krzek, M.; Stroobants, S.; Gelin, P.; De Malsche, W.; Maes, D. Influence of Centrifugation and Shaking on the Self-Assembly of Lysozyme Fibrils. *Biomolecules* **2022**, *12*, 1746, doi:10.3390/biom12121746.
299. Hill, E.K.; Krebs, B.; Goodall, D.G.; Howlett, G.J.; Dunstan, D.E. Shear flow induces amyloid fibril formation. *Biomacromolecules* **2006**, *7*, 10-13, doi:10.1021/bm0505078.
300. Dunstan, D.E.; Hamilton-Brown, P.; Asimakis, P.; Ducker, W.; Bertolini, J. Shear flow promotes amyloid-beta fibrilization. *Protein Eng Des Sel* **2009**, *22*, 741-746, doi:10.1093/protein/gzp059.
301. Chaari, A.; Fahy, C.; Chevillot-Biraud, A.; Rholam, M. Insights into Kinetics of Agitation-Induced Aggregation of Hen Lysozyme under Heat and Acidic Conditions from Various Spectroscopic Methods. *PLoS One* **2015**, *10*, e0142095, doi:10.1371/journal.pone.0142095.

302. Teoh, C.L.; Bekard, I.B.; Asimakis, P.; Griffin, M.D.; Ryan, T.M.; Dunstan, D.E.; Howlett, G.J. Shear flow induced changes in apolipoprotein C-II conformation and amyloid fibril formation. *Biochemistry* **2011**, *50*, 4046-4057, doi:10.1021/bi2002482.
303. Dunstan, I.B.B.a.D.E. The Effect of Shear Flow on Amyloid Fibril Formation and Morphology. In *Bio-nanoimaging: Protein Misfolding & Aggregation*, Uversky, V.N., Lyubchenko, Y.L., Eds.; Elsevier: Amsterdam, 2014; pp. 503-513.
304. Gospodarczyk, W.; Kozak, M. The severe impact of *in vivo*-like microfluidic flow and the influence of gemini surfactants on amyloid aggregation of hen egg white lysozyme. *RSC Adv* **2017**, *7*, 10973, doi:10.1039/c6ra26675d.
305. Mangione, P.P.; Esposito, G.; Relini, A.; Raimondi, S.; Porcari, R.; Giorgetti, S.; Corazza, A.; Fogolari, F.; Penco, A.; Goto, Y.; et al. Structure, folding dynamics, and amyloidogenesis of D76N beta2-microglobulin: roles of shear flow, hydrophobic surfaces, and alpha-crystallin. *J Biol Chem* **2013**, *288*, 30917-30930, doi:10.1074/jbc.M113.498857.
306. Dobson, J.; Kumar, A.; Willis, L.F.; Tuma, R.; Higazi, D.R.; Turner, R.; Lowe, D.C.; Ashcroft, A.E.; Radford, S.E.; Kapur, N.; et al. Inducing protein aggregation by extensional flow. *Proc Natl Acad Sci U S A* **2017**, *114*, 4673-4678, doi:10.1073/pnas.1702724114.
307. Herrera-Rodríguez, A.M.; Dasanna, A.K.; Daday, C.; Cruz-Chú, E.R.; Aponte-Santamaría, C.; Schwarz, U.S.; Gräter, F. The role of flow in the self-assembly of dragline spider silk proteins. *Biophys J* **2023**, *122*, 4241-4253, doi:10.1016/j.bpj.2023.09.020.
308. Almohammadi, H.; Bagnani, M.; Mezzenga, R. Flow-induced order-order transitions in amyloid fibril liquid crystalline tactoids. *Nat Commun* **2020**, *11*, 5416, doi:10.1038/s41467-020-19213-x.
309. Majka, Z.; Kwiecien, K.; Kaczor, A. Vibrational Optical Activity of amyloid fibrils. *Chempluschem* **2024**, e202400091, doi:10.1002/cplu.202400091.
310. Kleiner-Grote, G.R.M.; Risse, J.M.; Friehs, K. Secretion of recombinant proteins from *E. coli*. *Eng Life Sci* **2018**, *18*, 532-550, doi:10.1002/elsc.201700200.
311. Inoue, H.; Nojima, H.; Okayama, H. High efficiency transformation of *Escherichia coli* with plasmids. *Gene* **1990**, *96*, 23-28, doi:10.1016/0378-1119(90)90336-p.
312. Schimek, C.; Egger, E.; Tauer, C.; Striedner, G.; Brocard, C.; Cserjan-Puschmann, M.; Hahn, R. Extraction of recombinant periplasmic proteins under industrially relevant process conditions: Selectivity and yield strongly depend on protein titer and methodology. *Biotechnol Prog* **2020**, *36*, e2999, doi:10.1002/btpr.2999.
313. Mital, S.; Christie, G.; Dikicioglu, D. Recombinant expression of insoluble enzymes in *Escherichia coli*: a systematic review of experimental design and its manufacturing implications. *Microb Cell Fact* **2021**, *20*, 208, doi:10.1186/s12934-021-01698-w.